Investigation on solvometallurgical processes for extraction of metals from sulfides

Kurniawan Kurniawan, Sookyung Kim, Mooki Bae, Alexandre Chagnes, Jae-Chun Lee

Minerals Engineering 218 (2024) 109005

Contents lists available at ScienceDirect

Minerals Engineering

journal homepage: www.elsevier.com/locate/mineng

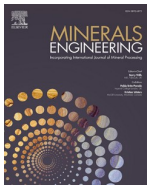

Investigation on solvometallurgical processes for extraction of metals from sulfides

Kurniawan Kurniawan [a,b], Sookyung Kim [a,b,*], Mooki Bae [b], Alexandre Chagnes [c], Jae-chun Lee [a,b,*]

[a] Resources Recycling, University of Science and Technology, Daejeon 34113, Republic of Korea
[b] Resources Utilization Research Division, Korea Institute of Geoscience and Mineral Resources (KIGAM), Daejeon 34132, Republic of Korea
[c] Université de Lorraine, CNRS, GeoRessources, F- 54000 Nancy, France

ARTICLE INFO

Keywords:
Solvometallurgy
Metal sulfides
Dissolution mechanism
Sustainable extraction

ABSTRACT

Copper, nickel, iron, zinc, lead, and molybdenum are among the important metals commonly found as sulfide minerals in nature. Some of these metals are also found as sulfides in intermediate products like matte and mixed sulfide precipitates (MSP). The extraction processes of these metals from their sulfide forms through either pyrometallurgy or hydrometallurgy encounter various challenges. This study aimed to explore the viability of solvometallurgical processes (solvoleaching) as potential alternatives for the extraction of these metals from their sulfides (CuS, Ni_3S_2, FeS, ZnS, PbS and MoS_2). The solvometallurgical processes employed a range of solvoleaching systems, such as D2EHPA+MnO_2+H_2O, ammoniacal solvoleaching comprising of LIX 84-I+NH_4OH+H_2O_2, HCl-equilibrated TBP (TBP-HCl) and EG (ethylene glycol)-based solvents containing each of HCl, $FeCl_3$, ChCl and NH_4Cl. The solvoleaching mechanism of the metal sulfides in each solvoleaching system was discussed. The results were corroborated with thermodynamic tools like Eh-pH diagrams, Gibbs free energy change, and solvation properties of the metal ions, as well as the hard and soft acid-base (HSAB) theory. Analyses of the resulting leach solutions, utilizing suitable analytical techniques such as UV–Vis spectroscopy and FTIR, provided additional support for the results. A comparison made between the solvoleaching and classical aqueous leaching, showing comparable results, indicated the viability of solvoleaching processes as alternatives for the sustainable extraction of these metals from their sulfides.

1. Introduction

Many important metals, including copper, nickel, iron, zinc, lead, molybdenum, etc. are commonly found in nature as sulfide minerals/ores. In fact, about half (or even higher) of the global production of these metals is derived from sulfide minerals/ores (Nayak et al., 2022; Faris et al., 2023; Zhao et al., 2022). Traditionally, the extraction of metals from sulfide minerals/ores has relied on pyrometallurgial processes, particularly via roasting and smelting, to produce matte (Crundwell et al., 2011). The predominance of pyrometallurgical processes in sulfide mineral/ore processing is attributed to two primary factors: (i) the ease of concentrating sulfide minerals through flotation, thereby meeting the requirements for smelting operations, and (ii) the use of sulfur as fuel energy source during smelting (Peters, 1976). Following smelting, the produced matte typically undergoes refining processes, which often involve hydrometallurgical processes such as acid leaching (utilizing sulfate or chloride systems) or alkaline leaching (commonly ammoniacal processing). Notably, certain metals, such as lead and zinc, may require distinct pyrometallurgical pathways (Crundwell et al., 2011). Literature has provided extensive information on the scientific understanding and practical applications of pyrometallurgical processing of sulfide minerals (Crundwell et al., 2011; Nayak et al., 2022; Faris et al., 2023; Zhao et al., 2022). However, significant environmental pollution associated with roasting-smelting and the ongoing decline in the grade of sulfide ores render pyrometallurgical processes unsuitable for future extractive metallurgy.

The implementation of full hydrometallurgical processes (direct leaching) has been advancing in the processing of sulfide minerals/ores (Crundwell et al., 2011; Faris et al., 2023). The leaching of sulfide minerals/ores utilizes similar technologies to those used in the hydrometallurgical refining of matte, with the choice of leaching process being determined by the chemistry of the targeted metals. Leaching can

* Corresponding authors.
E-mail addresses: skkim@kigam.re.kr (S. Kim), jclee@kigam.sci.kr (J.-c. Lee).

https://doi.org/10.1016/j.mineng.2024.109005
Received 17 April 2024; Received in revised form 27 August 2024; Accepted 17 September 2024
Available online 24 September 2024

be performed under either atmospheric or pressurized conditions (Crundwell et al., 2011; Faris et al., 2023), with the latter, often referred to as autoclave leaching, typically yielding good results. During leaching, sulfur undergoes various transformations, including conversion to sulfate, sulfamate, elemental sulfur, polysulfides, or occassionally H_2S (Kurniawan and Mubarok, 2018; Mubarok et al., 2018). The specific sulfur forms present during leaching depend on the conditions leaching conditions, but majority remains within the leaching system, rather than being released as gas. Hence, leaching processes of sulfide minerals/ores is often considered to be environmentally benign (Peters, 1976). Although, this does not universally hold true (Kadivar et al., 2024). Despite demonstrating promising results in laboratory-scale experiments, successful commercialization of pressure leaching has been limited. The challenges include high capital and operational costs for autoclaves, complexities in operational and maintenance procedures, corrosion issues, energy demands, production of significant effluent, tailings and low-cost byproducts, etc. (Crundwell et al., 2011; Faris et al., 2023). Bio-assisted leaching, or bioleaching, which involves the assistance of microorganisms, has emerged as a promising alternative for the leaching of sulfide minerals/ores (Chaerun et al., 2023; Vera et al., 2022; Watling, 2006). This approach is particularly focused on treating low-grade sulfide minerals/ores (Mubarok et al., 2017; Panda et al., 2015).

Recently, a new class of leaching-based processes, known as solvometallurgy or solvoleaching, has attracted significant interest. Solvometallurgy (solvoleaching) represents an emerging branch of extractive metallurgy that employs non-aqueous or organic solvents for leaching processes (Binnemans and Jones, 2017). These non-aqueous or organic solvents can include polar organic solvents, organic extractants, ionic liquids (ILs) and deep eutectic solvents (DESs), which can be applied in their original forms or diluted in suitable diluents like nonpolar solvents (kerosene, for instance) or even water (but its volume should be below 50 vol%) (Binnemans and Jones, 2017; Li and Binnemans, 2021). These non-aqueous/organic solutions may be combined with active components like acids, alkalis, oxidants or ligands to increase their solvoleaching ability if needed (Li and Binnemans, 2021).

Indeed, non-aqueous/organic solvents possess unique features compared to classical aqueous solutions (Binnemans and Jones, 2017). Therefore, it is of great interest to examine their efficacy in the treatment of materials such as metal sulfides. Reported studies on the solvoleaching of metal sulfides has predominantly concentrated on the treatment of chalcopyrite by utilizing ionic solvents like ILs (Anggara et al., 2019; Carlesi et al., 2022; Li et al., 2020). Hence, there is a notable gap in understanding solvoleaching processes for Cu-Fe sulfides in comparison to other metals. Furthermore, it is crucial to prove the feasibility of employing other solvent systems in the solvoleaching process of metal sulfides. Hence, the main objective of this study is to evaluate the applicability of solvoleaching processes in the treatment of six important metals (copper, nickel, iron, zinc, lead, molybdenum) of their respective sulfide forms, namely CuS, Ni_3S_2, FeS, ZnS, PbS and MoS_2. The selection of these basic sulfide forms is intended to demonstrate the concept of solvoleaching for metal sulfides, thereby minimizing the influence of matrix effects or impurities. These metal sulfides are often found as sulfide minerals as well as in matte, making such a study relevant for the processing of these substances (actual sulfide forms). A range of solvoleaching systems were investigated, including acidic organophosphorus extractant, di-(2-ethylhexyl)phosphoric acid (D2EHPA) with MnO_2 as oxidant and addition of a small amount of water; chelating extractant, 2-hydroxylnonyl-acetophenon oxime (LIX 84-I) with a small amount of NH_4OH and H_2O_2 (also named as ammoniacal solvoleaching); HCl-equilibrated tri-butyl-phosphate (TBP); each of choline chloride (ChCl), ammonium chloride (NH_4Cl), hydrochloric acid (HCl) and iron(III) chloride ($FeCl_3$) dissolved in ethylene glycol (EG). These solvoleaching systems may possibly be used in the processes as mentioned above while also expecting some green impacts, making such discussion comprehensive. The solvoleaching mechanism of the metal sulfides is also discussed in some detail. The findings from this study aim to advance the development of solvoleaching processes for sulfide minerals/ores/compounds, providing a foundation for further research in this area.

2. Materials and methods

2.1. Materials

CuS (99.8 %, Alfa Caesar, USA), FeS (99.9 %, Sigma Aldrich, USA), MoS_2 (99.9 %, Duksan Reagents, Korea), Ni_3S_2 (99.7 %, Sigma Aldrich), PbS (99.9 %, Sigma Aldrich, USA) and ZnS (99.9 %, Sigma Aldrich, USA) were used as received. D2EHPA (97 %, Sigma Aldrich, USA) and LIX 84-I (96 %, BASF, Germany), diluted at desired concentrations in kerosene (Junsei, Japan), were used as extractants. MnO_2 (90 %, Junsei, Japan) was used as oxidant in the specified experiment when using D2EHPA as the lixiviant. NH_4OH (30 %, Daejung Chemical, Korea) was specifically added to LIX 84-I to examine the ammoniacal solvoleaching system-$\cdot H_2O_2$ (35 %, Samchun Chemical, Korea) was used as oxidant during ammoniacal solvoleaching experiments. TBP (99 %, Samchun Chemical, Korea) was equilibrated with HCl (35 %, Daejung, Korea) for 1 h; afterward, the two phases were separated and the obtained HCl-equilibrated TBP was used in the experiments. Specified amount of HCl, $FeCl_3$ (98 %, Samchun, Korea), ChCl (99 %, Samchun, Korea) and NH_4Cl (99 %, Duksan reagents, Korea) was dissolved in ethylene glycol/EG (99.5 %, Samchun, Korea). Lead acetate paper strip (Sigma Aldrich, Germany) was used to detect H_2S formation during the experiments. Reagent grade metal chloride salts like $CuCl_2$ (99 %, Sigma Aldrich, USA), $NiCl_2$ (99.9 %, Sigma Aldrich, USA), $ZnCl_2$ (99 %, Duksan reagents, Korea), $FeCl_2$ (99.9 %, Junsei, Japan), $FeCl_3$ and $PbCl_2$ (99 %, Samchun, Korea) were used to investigate their dissolution in selected solvent systems. To examine the solvoleaching of molybdenum, MoO_2 (99 %, Sigma Aldrich, USA) was used. H_2SO_4 (95 %, Junsei, Japan) was used for performing leaching in aqueous media to compare the hydrometallurgical route with the solvoleaching route.

2.2. Methods

- **Solvoleaching experiments**

The solvoleaching systems were investigated using the following protocols:

- 2.0 M of D2EHPA in kerosene with the addition of small amount of water (0.2 mL/20 mL of D2EHPA) and 7.5 g/L MnO_2
- 2.0 M LIX 84-I in kerosene, with addition of 0.3 mL NH_4OH and 0.3 mL H_2O_2 (per 20 mL of LIX 84I), quoted ammoniacal solvoleaching/LIX 84-I+NH_4OH+H_2O_2
- HCl-equilibrated TBP (un-diluted, quoted TBP-HCl)
- 2.0 M of each HCl/ChCl/NH_4Cl in EG, and
- 7.5 g/L $FeCl_3$ in EG

In all solvoleaching experiments, 0.2 g of a metal salt/metal sulfide was put into a 20 mL preheated solvent. The solvoleaching was carried out at 90 °C (except for the ammoniacal solvoleaching system which the experiment was performed at 25 °C) and 700 rpm stirring speed for 6 h. The same conditions were applied when dissolving metal salts except for the time of 1 h. The resulting leach solutions from D2EHPA, LIX 84-I and TBP systems were stripped using either 4.0 M H_2SO_4 or 4.0 M NH_4OH (all double-checked using 6.0 M HCl). The stripped solutions were then diluted properly using 5 vol% HNO_3 and then analyzed by inductively coupled plasma-atomic emission spectroscopy (ICP-AES, iCAP6000 series, Thermo Scientific, USA). The leach solutions obtained from solvoleaching using EG-based systems were also diluted using 5 vol% HNO_3. It may be noted that stripping/dilution steps of the resulting leach solutions were carried out right after the solvoleaching

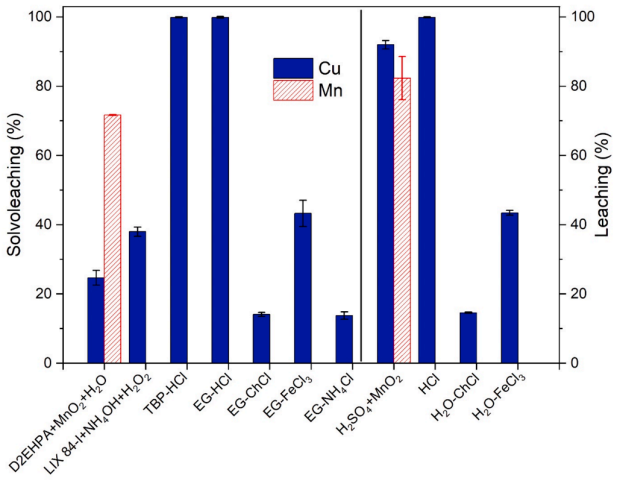

Fig. 1. Solvoleaching and aqueous leaching results of CuS (Conditions: 0.2 g of CuS in 20 mL of each solvent, which are 2.0 M D2EHPA + 0.2 mL water + 7.5 g/L MnO_2, 2.0 M LIX 84-I + 0.3 mL NH_4OH + 0.3 mL H_2O_2, undiluted TBP-HCl, 2.0 M EG-HCl, 2.0 M EG-ChCl, 2.0 M EG-NH_4Cl and EG with 7.5 g/L $FeCl_3$, 90 °C except for LIX 84-I (25 °C), 6 h, 700 rpm; the aqueous leaching was carried out under the same conditions).

experiments had finished to prevent precipitation prior to the cooling down. Each experiment was repeated three times, and average values reported are within < 5 % error. The solvoleaching efficiency was calculated according to Eq. (1); purity of the metal sulfides was also taken into account while calculating the efficiency.

$$\text{Solvoleaching}\,(\%) = \frac{m_{\text{leached}}}{m_{\text{initial}}} \times 100\% \quad (1)$$

where $m_{leached}$ and $m_{initial}$ are the amount of metal leached and the initial amount of metal in the metal sulfides, respectively.

The obtained leach solutions were characterized by Fourier transform infrared (FTIR, Nicolet iS5, Thermo Scientific, USA) and UV–Vis spectroscopy (Optizen POP, Korea).

- **Aqueous leaching experiments**

Leaching of the metal sulfides of interest was also carried out using classical aqueous systems for comparison. In a specific experiment, the metal sulfide was leached in a 2.0 M H_2SO_4 solution with the addition of 7.5 g/L MnO_2. In another experiment, 2.0 M HCl was used as the lixiviant. The leaching was also carried out using 7.5 g/L $FeCl_3$ and 2.0 M ChCl in water. All the other leaching conditions maintained were same as that of solvoleaching experiments.

3. Thermodynamics of metal sulfide systems

The Eh-pH diagram is a useful tool for predicting the stability of metals in contact with solutions of desired strength. The Eh-pH diagrams of Cu/Ni/Fe/Zn/Pb/Mo-S in H_2O system were constructed using HSC 6.0 software and are presented in **Supplementary Materials (SM)** Fig. S1–6. The diagrams illustrate the conditions under which the metals exist as soluble species, sulfides, hydroxides, and other forms. Additionally, the diagrams additionally depict the fate of sulfur, denoting whether it forms new solids like elemental sulfur (S^0), polysulfides, soluble sulfate (SO_4^{2-}) or S^{2-} ions under certain leaching conditions. Metal speciation diagrams as a function of pH and ligand concentrations (NH_3 and Cl) were also constructed using Medusa Software database. All these diagrams were employed to elucidate the phenomena during the solvoleaching processes.

4. Results and discussions

As mentioned earlier the reagent grade CuS, Ni_3S_2, FeS, ZnS, PbS and MoS_2 were used to investigate the applicability of various solvoleaching systems to treat metal sulfides. Results are presented and discussed, and are further supported by the analysis of the obtained leach solutions using FTIR and UV–Vis techniques (presented later).

4.1. Copper sulfide (CuS) dissolution

4.1.1. Solvoleaching of CuS

The solvoleaching results for CuS in various solvoleaching systems are presented in Fig. 1. Specific observation regarding H_2S formation and solution behaviors after cooling down to room temperature are summarized in Tables 1 and 2, respectively. For the system D2EHPA+MnO_2+H_2O, a Cu solvoleaching efficiency of 24.7 % (corresponding to Mn solvoleaching efficiency of 55.1 %) was achieved. In the process, D2EHPA functioned as the active component by providing

Table 1
Detection of H_2S formation during (a) solvoleaching and (b) aqueous leaching of metal sulfides.

(a)

Metal sulfides	D2EHPA+MnO_2 + H_2O	Ammoniacal solvoleaching	TBP-HCl	EG-HCl	EG-$FeCl_3$	EG-ChCl	EG-NH_4Cl
CuS	x	x	√ (initial time (30 min); small part)	x	√ (initial time (1 h))	√ (after 3 h)	x
Ni_3S_2	x	x	√	√	√	√ (small part)	x
FeS	√	x	√	√	x	√	√ (small part)
ZnS	√	x	√	√	√	√	√
PbS	√ (small part)	x	√	√	√	x	√
MoS_2	√	x	√	√	√	x	x

(b)

Metal sulfides	H_2SO_4 + MnO_2	HCl	H_2O-$FeCl_3$	H_2O-ChCl
CuS	x	x	√	√ (small part)
Ni_3S_2	x	√	√	√ (small part)
FeS	√	√	√	√
ZnS	√	√	√	√
PbS	√	√	√	x
MoS_2	√	√	√	x

Table 2
Coloration and precipitation behavior of resulting leach solutions from the solvoleaching of metal sulfides after cooling down to room temperature.

Metal sulfides	D2EHPA+MnO_2 + H_2O	Ammoniacal solvoleaching	TBP-HCl	EG-HCl	EG-$FeCl_3$	EG-ChCl	EG-NH_4Cl
CuS	Yellowish; no precipitation	Dark green; no precipitation	Yellowish; no precipitation – two separated phases	Yellowish green; no precipitation	Brown; precipitation (brown)	Green; precipitation (ultrafine, black)	Green; precipitation (deep-blue)
Ni_3S_2	Yellowish; no precipitation	Green; no precipitation	Yellowish; no precipitation – two separated phases	Green; no precipitation	Green; precipitation	No color; precipitation (ultrafine, black)	Light green; precipitation (ultrafine, black)
FeS	Yellowish; no precipitation	Black; precipitation (brown)	Yellowish; precipitation (brown)	Yellow; precipitation (brown)	Yellowish; precipitation (brown)	Yellow; precipitation (brown)	Yellowish; precipitation (brown)
ZnS	Yellowish; no precipitation	Brown; precipitation	No color; no precipitation – two separated phases	Light yellow; no precipitation	Yellowish; precipitation	No color; precipitation (white)	No color; precipitation (white)
PbS	Yellowish; precipitation	Yellowish brown; precipitation (black)	No color; precipitates (white)	Yellowish; precipitation (white)	Yellowish; precipitation (white)	No color; precipitation (ultrafine, black)	Yellowish; precipitation (black)
MoS_2	Yellowish; no precipitation	Yellowish; no precipitation	No color; no precipitation	Yellowish; no precipitation	Yellowish; precipitation (brown)	No color; no precipitation	No color; no precipitation

necessary protons (H^+) and a site for metal complexation (conjugated base of D2EHPA), MnO_2 as the oxidant (where Mn(IV) reduced to Mn (II)) and water as a catalyst to increase the solvoleaching performance. The solvoleaching reaction might occur according to Eq. (2). The calculated standard Gibbs free energy (ΔG^0) of the reaction between CuS, MnO_2 and H^+ is equal to –113.48 kJ/mol, which shows that the reaction is thermodynamically favorable. The formed cations experienced proton exchange with H^+ of D2EHPA molecule; the exchanged H^+ was used for further solvoleaching while the exchanged cations reacted with deprotonated D2EHPA molecule to form metal-D2EHPA complexes, according to Eqs. (3)–(4) (Devi, 2015; Ineza et al., 2022). Therefore, it is important to have an adequate ion exchange and metal-D2EHPA complexation to ensure the continuous solvoleaching process. These descriptions are further corroborated by FTIR and UV–Vis analysis. No precipitate formation was observed from the resulting leach solution (M−loaded D2EHPA), as both Cu^{2+} and Mn^{2+}-D2EHPA complexes so obtained are dissolved well in kerosene. Optimizing the solvoleaching process by adjusting MnO_2 dosage and extending the duration of solvoleaching could potentially enhance Cu solvoleaching efficiency further.

Solvoleaching of CuS with D2EHPA (proton donor, H^+) and MnO_2:

$$CuS_{(s)} + MnO_{2(s)} + 4H^+ \rightarrow Cu^{2+} + Mn^{2+} + S^0_{(s)} + 2H_2O_{(aq)}, \Delta G^0 = -113.48 \text{ kJ/mol} \quad (2)$$

$$Cu^{2+}_{(aq)} + 2(HA)_{2(org)} \rightleftarrows (CuA_2.(HA)_2)_{(org)} + 2H^+_{(aq)} \quad (3)$$

$$Mn^{2+}_{(aq)} + 3(HA)_{2(org)} \rightleftarrows (MnR_2.(HA)_4)_{(org)} + 2H^+_{(aq)} \quad (4)$$

Ammoniacal solvoleaching (LIX 84-I+NH_4OH+H_2O_2) resulted in the recovery of 38.0 % Cu. The solvoleaching process can be described as follows:

- CuS initially reacted with NH_4OH to form ammine complexes, $Cu(NH_3)^{2+}_n$ according to Eq. (5). The negative value of the standard Gibbs free energy confirms that the reaction can occur from the thermodynamic point of view ($\Delta G^0 = -1227.66$ kJ by considering n = 3 for the Gibbs energy calculation for the sake of simplicity). The reaction reported in Eq. (5) could indeed occur since H_2O_2 was added into the solvoleaching system, thereby establishing the oxidizing alkali conditions necessary for $Cu(NH_3)^{2+}_n$ formation.
- The Cu^{2+} ions from $Cu(NH_3)^{2+}_n$ complexes were simultaneously extracted by LIX 84-I to form Cu-LIX 84-I complex and release NH_3 back for the leaching reaction, according to Eq. (6). Therefore, Cu solvoleaching could continue even though only a small volume of NH_4OH was added.

CuS − Ammoniacal solvoleaching system:

$$CuS_{(s)} + NH_4OH_{(aq)} + H_2O_{2(aq)} \rightarrow Cu(NH_3)^{2+}_{(aq)} + SO^{2-}_{4(aq)} + 7H_2O_{(aq)}, \Delta G^0 = -1227.6 \text{ kJ/mol} \quad (5)$$

$$Cu(NH_3)^{2+}_{(aq)} + 2(RH)_{2(org)} \rightleftarrows (CuR.(RH)_2)_{(org)} + NH_3 + 2NH^+_4 \quad (6)$$

As the solvoleaching proceeded, NH_3 would be equilibrated by LIX 84-I and all H_2O_2 molecules were consumed; therefore, limiting the Cu solvoleaching to an extent. No precipitate was observed for the same reasons as those given previously CuS solvoleaching by D2EHPA.

Quantitative Cu solvoleaching was achieved using HCl-based systems, namely TBP-HCl and EG-HCl. In the TBP-HCl system, a slight darkening of lead acetate paper strips was observed within first 30 min of solvoelaching, whereas no such occurrence was observed in the EG-HCl system. This indicates minimal H_2S formation during CuS solvoleaching in the TBP-HCl system. This limited H_2S formation can be attributed to the strong acidic nature of the TBP-HCl solution, which facilitates the reaction of CuS according to Eq. (7) (refer to Case 1.2: Strong acid leaching in **Fig. S1**). At a low water level (non-aqueous solvent) and high chloride concentration, as in the case of TBP-HCl and EG-HCl, chloride activity increases to augment the probability of Cl_2 formation via Eq. (8) (Li et al., 2018; Nakagawa et al., 2018; Nguyen et al., 2022). This Cl_2 oxidized H_2S to S^0, according to Eq. (9); this is the reason that H_2S formation stopped after certain time (30 min) in TBP-HCl system. In the EG-HCl system, the absence of H_2S formation can be attributed to the solvation properties of EG, which has two HBD and HBA counts. This solvation capacity may influence the reaction kinetics, resulting in the suppression of H_2S formation, as described by Eq. (9).

$$CuS_{(s)} + 2H^+_{(org)} + 2Cl^-_{(org)} \rightarrow CuCl_{2(org)} + H_2S_{(g)} \quad (7)$$

$$Cl\bullet_{(org)} + Cl\bullet_{(org)} \rightarrow Cl_{2(g)} \quad (8)$$

$$H_2S_{(g)} + Cl_{2(g)} \rightarrow S^0_{(s)} + 2HCl \quad (9)$$

The presence of Cu^{2+} species in TBP and EG was also confirmed by the FTIR and UV–Vis analysis, which will be presented later. Uniquely, after storing the resulting TBP-HCl leach solution at room temperature for 1 h, two distinct phases were observed: a small volume of a green solution, indicating the presence of Cu-chloro complexes, and a yellowish organic phase. This did not happen to EG-HCl solution. This observation highlights the differences in solvation capacity between TBP (which has zero HBD and four HBA counts) and EG. A similar effect was reported by Palden et al. (2019). An alternative explanation could be that HCl, which is not involved or weakly solvated in the TBP-HCl system, would collapse during storing to create a very high HCl solution to

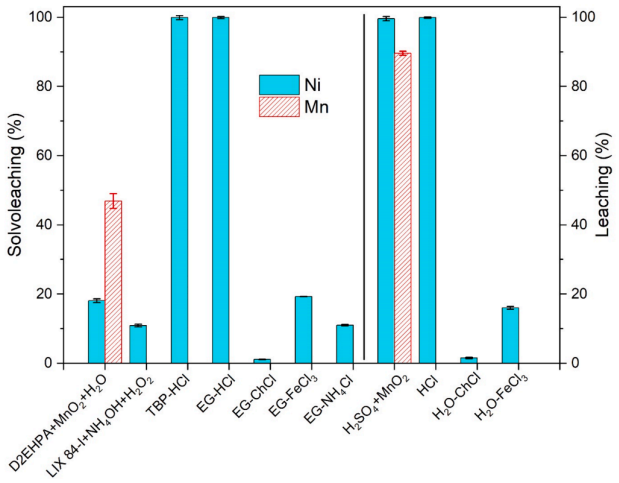

Fig. 2. Solvoleaching and aqueous leaching results of Ni_3S_2 (Conditions: 0.2 g of Ni_3S_2 in 20 mL of each solvent, which are 2.0 M D2EHPA + 0.2 mL water + 7.5 g/L MnO_2, 2.0 M LIX 84-I + 0.3 mL NH_4OH + 0.3 ML H_2O_2, undiluted TBP-HCl, 2.0 M EG-HCl, 2.0 M EG-ChCl, 2.0 M EG-NH_4Cl and EG with 7.5 g/L $FeCl_3$, 90 °C except for LIX 84-I (25 °C), 6 h, 700 rpm; the aqueous leaching was carried out under the same conditions).

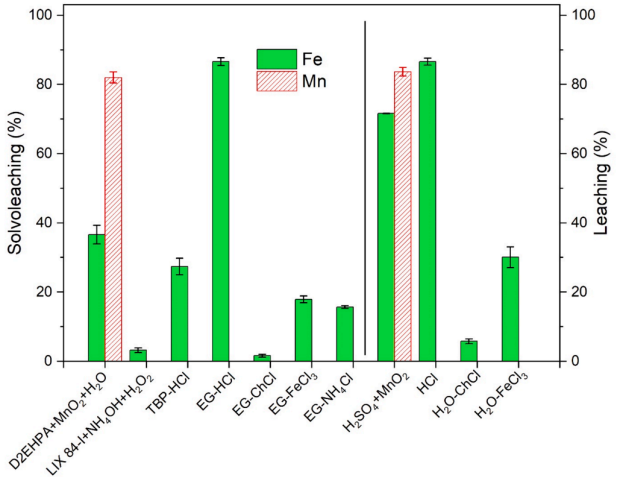

Fig. 3. Solvoleaching and aqueous leaching results of FeS (Conditions: 0.2 g of FeS in 20 mL of each solvent, which are 2.0 M D2EHPA + 0.2 mL water + 7.5 g/L MnO_2, 2.0 M LIX 84-I + 0.3 mL NH_4OH + 0.3 mL H_2O_2, undiluted TBP-HCl, 2.0 M EG-HCl, 2.0 M EG-ChCl, 2.0 M EG-NH_4Cl and EG with 7.5 g/L $FeCl_3$, 90 °C except for LIX 84-I (25 °C), 6 h, 700 rpm; the aqueous leaching was carried out under the same conditions).

partially strip the loaded Cu^{2+} from TBP.

Using other EG-based systems like EG-ChCl, and EG-$FeCl_3$, the Cu solvoleaching efficiencies were 14.1 % and 43.3 %, respectively. H_2S was detected in both solvoleaching systems. For the EG-ChCl system, the H_2S formation was likely because the solvent tended to form an acidic deep eutectic solvents (ADES) (Qin et al., 2020) and the reducing nature of this DES (Peeters et al., 2020). In this system, EG acts as a proton donor (H^+) while ChCl serves as a chloride donor (Cl^-) (Peeters et al., 2022), facilicating the solvoleaching of CuS according to Eq. (7). However, the limited chloride concentration in the solvent resulted in the negligible H_2S oxidation.

The solvoleaching of CuS in EG-$FeCl_3$ could also proceed according to Eq. (7). However, H_2S formation only occurred during the initial

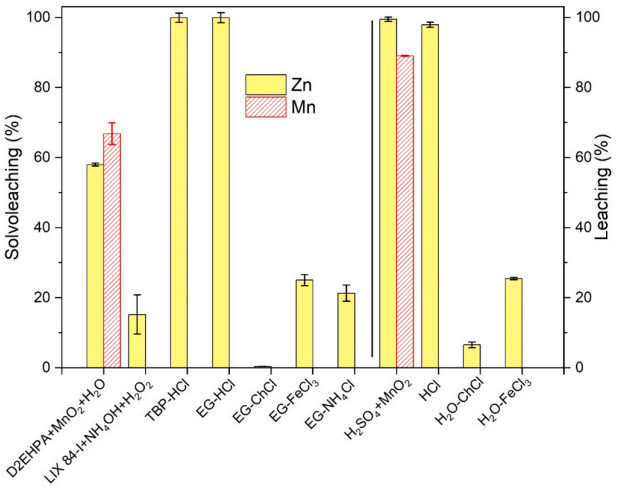

Fig. 4. Solvoleaching and aqueous leaching results of ZnS (Conditions: 0.2 g of ZnS in 20 mL of each solvent, which are 2.0 M D2EHPA + 0.2 mL water + 7.5 g/L MnO_2, 2.0 M LIX 84-I + 0.3 mL NH_4OH + 0.3 mL H_2O_2, undiluted TBP-HCl, 2.0 M EG-HCl, 2.0 M EG-ChCl, 2.0 M EG-NH_4Cl and EG with 7.5 g/L $FeCl_3$, 90 °C except for LIX 84-I (25 °C), 6 h, 700 rpm; the aqueous leaching was carried out under the same conditions).

Table 3
Results of solvoleaching of PbS and MoO_2 and aqueous leaching of PbS and MoS_2. The solvoleaching of MoS_2 did not occur in any solvent systems, and thus same is not presented in the table. (Conditions: 0.2 g of PbS/MoS_2/MoO_2 in 20 mL of each solvent, which are 2.0 M D2EHPA+0.2 mL water + 7.5 g/L MnO_2, 2.0 M LIX 84-I+0.3 mL NH_4OH+0.3 mL H_2O_2, undiluted TBP-HCl, 2.0 M EG-HCl, 2.0 M EG-ChCl, 2.0 M EG-NH_4Cl and EG with 7.5 g/L $FeCl_3$, 90 °C except for LIX 84-I (25 °C), 6 h, 700 rpm; the aqueous leaching was carried out under the same conditions).

Solvent systems	Solvoleaching (%)		Aqueous leaching system	Leaching (%)	
	Pb	Mo from MoO_2		Pb	Mo from MoS_2
D2EHPA+MnO_2 + H_2O	30.9 ± 3.9 (61.3 ± 1.84)*	–	H_2SO_4 + MnO_2	○ (0.01), (83.5 ± 0.4)*	19.8 ± 2.4 (85.6 ± 4.8)*
Ammoniacal solvoleaching	16.5 ± 0.9	29.0 ± 2.2	HCl	○ (26.5 ± 4.5)	0.2
TBP-HCl	○	–	H_2O-$FeCl_3$	○ (4.72 ± 4.3)	0.05
EG-HCl	○ (15.8 ± 0.3)	46.2 ± 3.2	H_2O-ChCl	○ (2.79 ± 0.4)	0.03
EG-$FeCl_3$	○ (3.9 ± 0.7)	–			
EG-ChCl	○ (2.2 ± 0.4)	18.1 ± 0.5			
EG-NH_4Cl	○ (1.0 ± 0.8)	0.2 ± 0.1			

()* = Mn solvoleaching/leaching.
() = Percentage of remaining Pb in the solvents.
○ = precipitation occurred during the solvoleaching/leaching.
– = not tested.

period (~1h), likely while iron was still in its highest valence state (Fe^{3+}). As the solvoleaching proceeded, Fe^{3+} ions oxidized H_2S to S^0 while itself being reduced to Fe^{2+} (Eq. (10)) (Zheng et al., 2019). In particular, these reactions (7 and 10) are possible considering the fairly good degree of $FeCl_3$ solvation in EG (**Table S1**). However, precipitates were observed from the resulting leach solution after storing at room temperature for 24 h. This precipitation reaction may arise from the

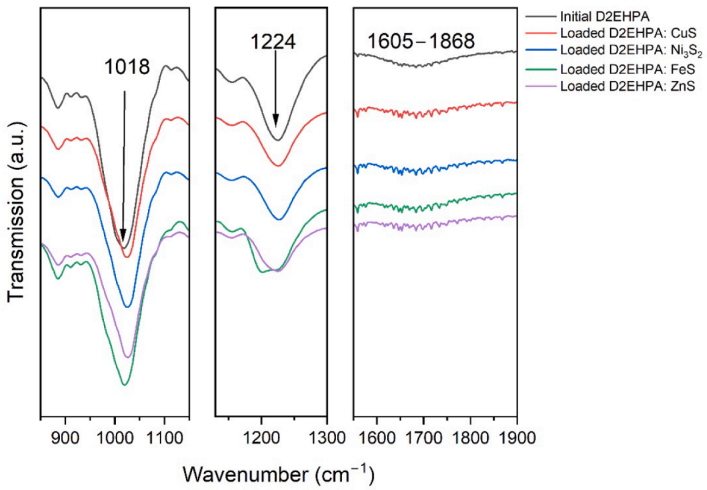

(a)

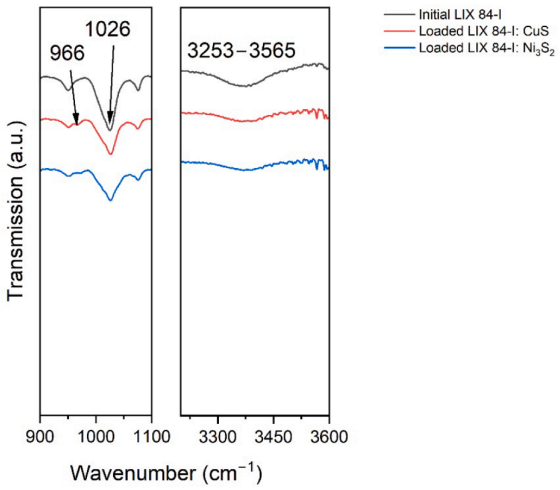

(b)

Fig. 5. FTIR spectra of leach solutions from solvoleaching using (a) D2EHPA, (b) LIX 84-I, (c) TBP, (d) EG-HCl, (e) EG-ChCl, (f) EG-$FeCl_3$, and (g) EG-NH_4Cl. The full spectra for each solvoleaching system are provided in Fig. S7.

limited solubility of Fe^{2+} in EG (strongly in accordance to the HSAB theory, wherein Fe^{2+} being a borderline acid, and solvation properties of Fe^{2+}, as presented in **Table S2**), or reduced solubility of metal chlorides in EG at lower temperatures (**Table S1**).

$H_2S_{(g)} + 2Fe^{3+}_{(org)} \rightarrow S^0_{(s)} + 2Fe^{2+}_{(org)} + 2H^+_{(org)}$ (10).

In the EG-NH_4Cl system, only 13.8 % Cu solvoleaching was achieved, and no H_2S was formed. The absence of H_2S formation can be attributed the formation of sulfate ions instead, as described in Eq. (5). However, deep-blue precipitates, probably $Cu(NH_3)_x(Cl/SO_4)_y$ salts (Nicol, 2018), were formed after the leach solution was cooled and stored for 24 h. This suggests that high temperatures are necessary to maintain the solubility of metal-ammine complexes in the EG solvent. Another possible explanation relates to the chemistry between Cl^- and the formed SO_4^{2-}. These two anions have different hydration energies ($\Delta_{hyd}G^0_{298K}$ SO_4^{2-} = –1080 kJ/mol, $\Delta_{hyd}G^0_{298K}$ Cl^- = –340 kJ/mol (Marcus, 1991)), which might influence the chemistry of the solution. This was further supported by the absence of precipitates in the resulting EG-NH_4Cl-$CuCl_2$ solution.

4.1.2. *Aqueous leaching of CuS*

Cu leaching efficiency from CuS by 2.0 M HCl, 2.0 M H_2SO_4 in the presence of 7.5 g/L MnO_2 as oxidant, 7.5 g/L $FeCl_3$ and 2.0 M ChCl was ~ 99.9 %, 92.0 % (corresponding to 82.3 % Mn leaching), 43.5 %, and 14.7 %, respectively (Fig. 1). The higher leaching efficiency obtained in H_2SO_4 compared to D2EHPA, under the same molarity and oxidant (MnO_2) conditions, is attributed to the more availability of H^+ ions provided by H_2SO_4, which facilitates the leaching reactions more effectively. Additionally, it also follows a simpler leaching mechanism when using H_2SO_4. The leaching using other aqueous systems demonstrated comparable results to those of solvoleaching systems. Yet another interesting observation made from the resulting leach solutions

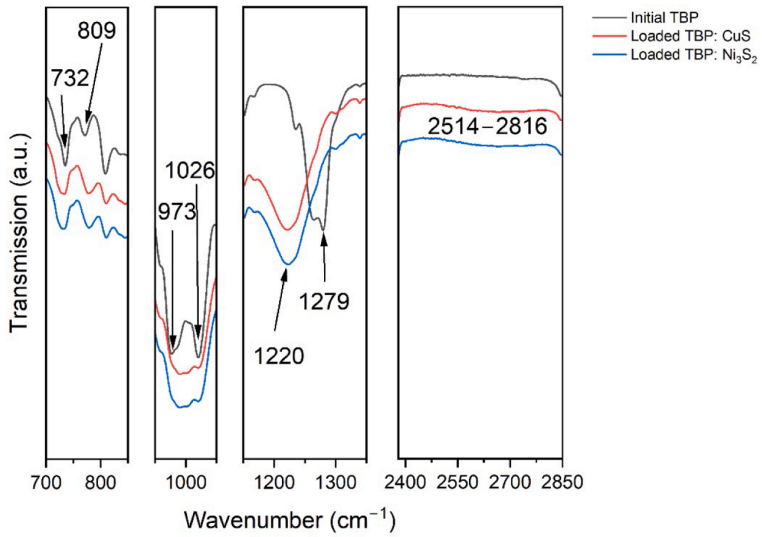

(c)

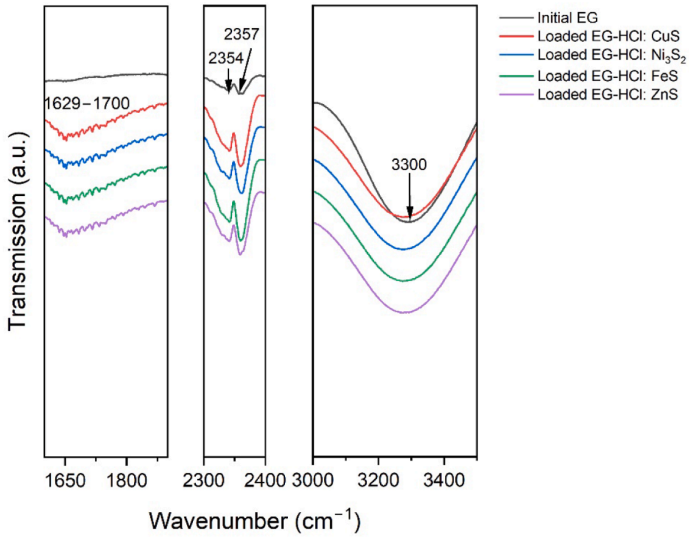

(d)

Fig. 5. (*continued*).

after aqueous leaching was that no precipitates were observed in any leaching systems. Only the leach solution of aqueous ChCl showed a cloudy/hazy solution after it was cooled down and stored for 24 h, which was probably related to the decrease of ChCl solubility in water at low temperature or due to the highly hydroscopic property of ChCl. This case, however, did not occur with EG-ChCl solution. From the comparable leaching results obtained, it can be said that solvoleaching is an alternate for the aqueous leaching of CuS.

4.2. Nickel sulfide dissolution (Ni_3S_2)

4.2.1. Solvoleaching of Ni_3S_2

The solvoleaching results for Ni from Ni_3S_2 are shown in Fig. 2, with the analysis of resulting leach solutions using FTIR and UV–Vis to confirm such occurrences (presented later). During the solvoleaching of Ni_3S_2 with D2EHPA+MnO_2 + H_2O, 18.1 % of Ni and 46.9 % of Mn were extracted, consistent with the oxidative solvoleaching equilibrium described in Eq. (11). The same equilibrium as that observed for the solvoleaching of CuS has happened here. The lower efficiency of Ni solvoleaching compared to that of copper can be attributed to the higher hydrophilicity of Ni^{2+} to limit its mobility towards D2EHPA, as

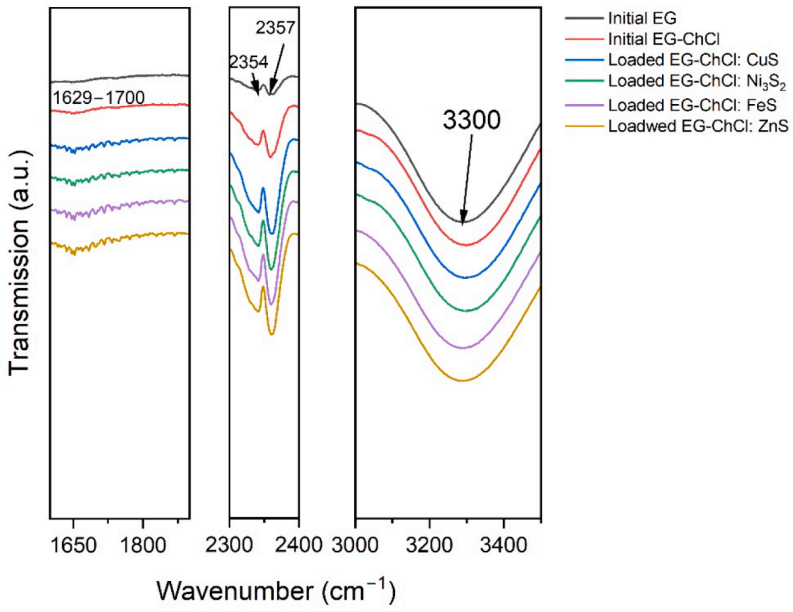

(e)

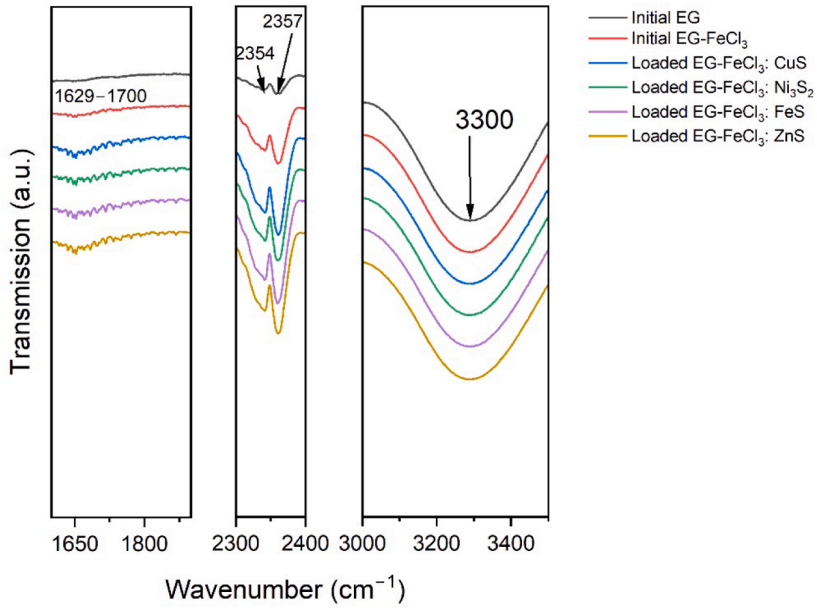

(f)

Fig. 5. (*continued*).

indicated by its solvation properties in Table S2. Additionally, the stability domain of Ni_3S_2 is located at negative potentials (reductive conditions) in the Eh-pH diagram (Fig. S2). This suggests the need for further oxidation to convert it into Ni^{2+} species.

Solvoleaching of Ni_3S_2 with H^+ (from D2EHPA) in presence of MnO_2:

$$Ni_3S_2 + 12H^+ + 3MnO_2 \rightarrow 3Ni^{2+} + 3Mn^{2+} + 2S^0 + 6H_2O, \Delta G^0_{298K} = -632.0\ kJ/mol \quad (11)$$

The recovery of Ni from Ni_3S_2 has also been recorded in ammoniacal solvoleaching system as nickel has the capability to form Ni-ammine complexes (Fig. S2) according to Eq. (12). However, the solvoleaching yield of nickel was only 10.9 %, which followed the same attributes as

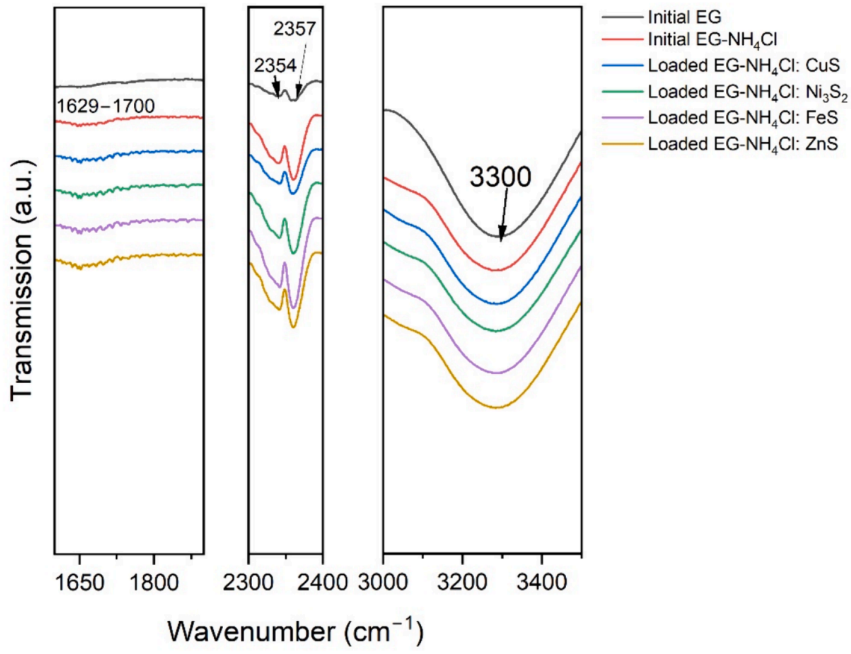

(g)

Fig. 5. (*continued*).

above regarding the nature and properties of Ni^{2+} and the stability domain of Ni_3S_2 at reductive conditions.

Ni_3S_2 – Ammoniacal solvoleaching system:

$$Ni_3S_{2(s)} + 2NH^{+}_{4(aq)} + 7NH_{3(aq)} + 4.5O_{2(g)} \rightarrow 3Ni(NH_3)^{2+}_{6(aq)} + H_2O_{(aq)} + 2SO^{2-}_{4(aq)}, \Delta G^{0}_{298K} = -1658.2\ kJ/mol \quad (12)$$

$$Ni(NH_3)^{2+}_{6(aq)} + 2(RH)_{2(org)} \rightleftarrows (NiR.(RH)_2)_{(org)} + NH_{3(aq)} + 2NH^{+}_{4(aq)} \quad (13)$$

In the TBP-HCl and EG-HCl systems, nearly quantitative solvoleaching of Ni from Ni_3S_2 was achieved. H_2S formation was observed in both systems, consistent with the strong acid leaching equilibrium described in Eq. (14) and in accordance with the Eh-pH diagram showing the stability domain of Ni_3S_2 (**Fig. S2**). For the TBP-HCl system, two distinct phases were observed after cooling the solution: a green aqueous phase and a light yellowish organic phase. The volume of this aqueous phase was higher than that observed for Cu. Specifically, only 11.8 % of the leached nickel remained in the TBP phase, whilst the majority of the leached nickel was found in the aqueous phase. This behavior could still due to the higher hydrophilicity of Ni^{2+}, which limits its solubility in TBP, as confirmed by the dissolution of $NiCl_2$ salt in TBP (**Table S1**). In contrast, the EG-HCl leach solution remained as a single phase even after cooling and storing for 24 h which is explained by the solvating properties of EG.

Solvoleaching of Ni_3S_2 in TBP-HCl and EG-HCl:

$$Ni_3S_{2(s)} + 6HCl_{(org)} \rightarrow 3NiCl_{2(org)} + H_{2(g)} + 2H_2S_{(g)} \quad (14)$$

The Ni solvoleaching efficiencies in EG-$FeCl_3$, EG-ChCl and EG-NH_4Cl systems were 19.3 %, 1.1 % and 11.0 %, respectively. The notably low Ni solvoleaching effiency in the EG-ChCl can be attributed to the reductive nature of the solvent (Peeters et al., 2022) (**Fig. S2**). H_2S formation was detected, although the color change of the lead acetate strip paper only happened partially in accordance with the low solvoleaching yield. Some ultrafine black precipitates were observed after cooling the solution, which was likely due to transformation of Ni_3S_2 into another intermediate sulfides like Ni_3S_4 or Ni_9S_8, following the reduction reactions (Yan et al., 2017).

In the EG-$FeCl_3$ and EG-NH_4Cl systems, the presence of Fe^{3+} and NH_4^+ likely enhanced the solvoleaching efficiency by facilitating the oxidation of Ni_3S_2 to Ni^{2+}. However, both systems exhibited the formation of ultrafine precipitates. In the EG-NH_4Cl, ultrafine black precipitates formed can be attributed to the complex oxidizing behavior of Ni_3S_2 in the limited ammoniacal system (**Fig. S2**). Meanwhile, brown precipitates were observed from the resultant leach solution of EG-$FeCl_3$, attributed to the same reason as the case of CuS solvoleaching related to limited solubility of Fe^{2+} as a borderline acid (according to the HSAB theory) in EG and its solvation properties (**Table S2**).

4.2.2. *Aqueous leaching of Ni_3S_2*

Ni leaching with 2.0 M H_2SO_4 + 7.5 g/L MnO_2 and 2.0 M HCl could reach almost quantitative (Fig. 2). The Ni leaching with aqueous solution of $FeCl_3$, however, was slightly lower (16.0 %) than with EG-$FeCl_3$ likely due to the hydration of Cl^- ions in water; this hydration suppressed the interaction between the metal ions and chloride that would form complexes (Nguyen et al., 2022). Still is limited of Ni leaching (only 1.6 %) in aqueous ChCl.

4.3. *Iron sulfide dissolution (FeS)*

4.3.1. *Solvoleaching of FeS*

The solvoleaching results of FeS depicted in Fig. 3, are discussed as follows. The solvoleaching of FeS using D2EHPA+MnO_2 + H_2O achieved the dissolution of 36.6 % Fe and 82.0 % of Mn, as described by Eq. (15). D2EHPA preferentially forms complexes with Fe^{3+} (or its $FeOH^{2+}$ form) rather than Fe^{2+} (Gutmann, 1968). The presence of MnO_2 and water, which reacts with D2EHPA to produce •OH or •O_2H, likely facilitates the oxidation of Fe^{2+} from FeS to Fe^{3+}/$FeOH^{2+}$ species (Eqs. (16)–(18)), thus enabling for the solvoleaching process through Fe(III)-D2EHPA complexation. This was confirmed by the FTIR and UV–Vis analysis presented later. H_2S formation was observed during solvoleaching but H_2S formation mechanisms are complex due to the

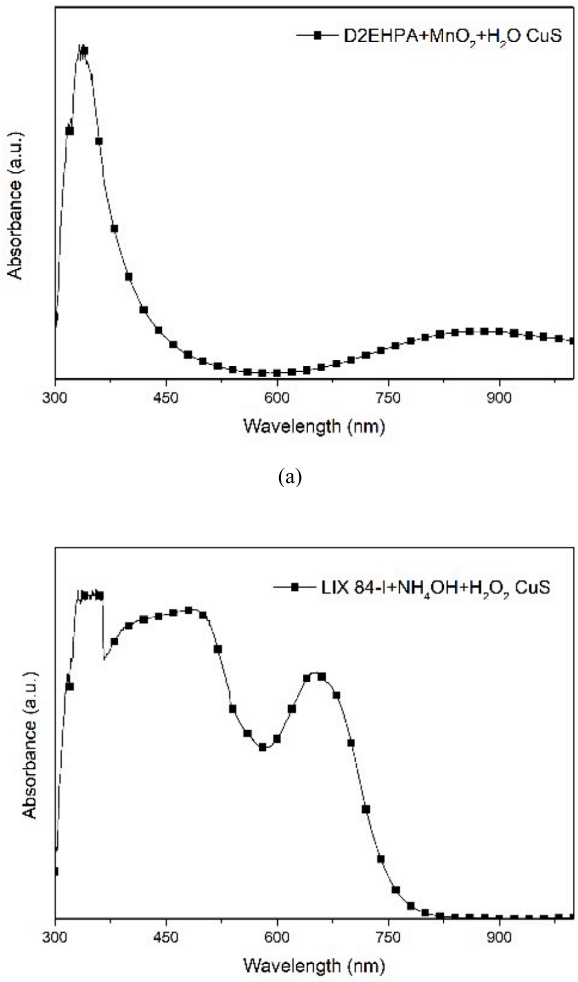

Fig. 6. UV–Vis spectra of Cu-containing solutions from the solvoleaching systems: (a) D2EHPA + MnO_2, (b) LIX 84-I + NH_4OH + H_2O_2, (c) TBP-HCl, (d) EG-HCl, (e) EG-$FeCl_3$, (f) EG-ChCl and (d) EG-NH_4Cl (solvoleaching conditions were mentioned in the text).

intricate chemistry involving Fe-S-MnO_2 interactions (Toro et al., 2021)) and the cyclic chemistry of sulfur when interacting with MnO_2 and added water (Eqs. (18)–(19)) (Schippers and Jørgensen, 2001). Additionally, the hard Lewis acid nature of Fe^{3+} ions (Gutmann, 1968) might affect the solvoleaching chemistry. These occurrences (oxidation of Fe^{2+} to Fe^{3+} by MnO_2 (Eq. (16)) and the cyclic chemistry of sulfur (Eqs. (19)–(20)) may be, therefore, the reasons of higher Mn solvoleaching when being suspended with FeS compared to other sulfides.

Solvoleaching of FeS with $[H]^+$ (from D2EHPA) and MnO_2:

$$FeS+4H^{+}+MnO_2 \rightarrow Fe^{2+}+Mn^{2+}+S^0+2H_2O, \Delta G^{0}_{298K}=-224.7\ \text{kJ/mol} \quad (15)$$

$$2Fe^{2+}+MnO_2+4H^{+}\rightarrow 2Fe^{3+}+Mn^{2+}+2H_2O, \Delta G^{0}_{298K}=-99.5\ \text{kJ/mol} \quad (16)$$

$$Fe^{2+}+\bullet OH\rightarrow Fe^{3+}+OH^{-} \quad (17)$$

$$Fe^{2+}+\bullet O_2H\rightarrow Fe^{3+}+HO_2^{-} \quad (18)$$

Cyclic chemistry of sulfur and MnO_2:

$$4S^0+4H_2O\rightarrow 3H_2S+SO_4^{2-}+2H^{+} \quad (19)$$

$$3H_2S+3MnO_2\rightarrow 3S^0+3Mn^{2+}+6OH^{-} \quad (20)$$

Iron recovery in the ammoniacal solvoleaching system was only 3.2 %. The low effectiveness of the ammoniacal solvoleaching system can be attributed to the thermodynamics of the Fe-NH_3 system (**Fig. S3**). During the ammoniacal solvoleaching process, H_2O_2 was introduced to oxidize Fe^{2+} into Fe^{3+}. However, Fe^{3+} had a low propensity to form ammine complexes, since it forms stable species like iron hydroxides/oxides (e.g., FeOOH, Fe_2O_3).

The iron solvoleaching efficiency in the TBP-HCl system was only 27.4 %, which is lower than the values obtained for Cu or Ni solvoleaching. The resulting leach solution was yellowish, and sludge was formed after cooling and storing the solution for 24 h. This is likely due to the low solubility of Fe^{2+} in TBP. Such an observation may be explained by the HSAB theory, as Fe^{2+} is a weak Lewis acid that exhibit lower coordination with TBP (Gutmann, 1968). This is consistent with the result observed when $FeCl_2$ was dissolved in TBP (**Table S1**). The oxidation state of iron was only Fe^{2+}, presented later in the UV–Vis

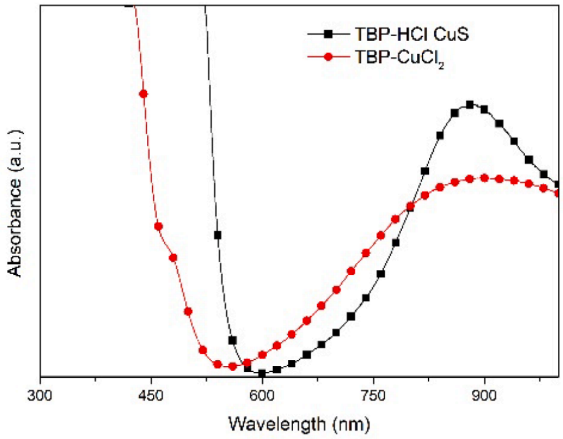

(c)

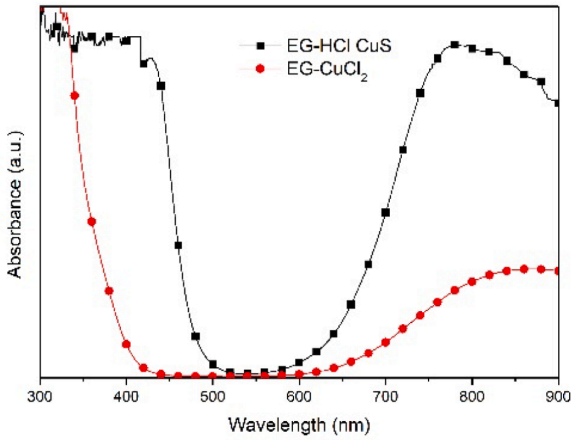

(d)

Fig. 6. (*continued*).

analysis, as no oxidant was added during solvoleaching (and water from the equilibrated HCl was limited). The limited Fe^{2+} solubility in the solvent could also explain the precipitation occurring when EG was used as solvent (regardless the accompanying active components like HCl (Fe solvoleaching = 86.6 %), $FeCl_3$ (Fe solvoleaching = 17.9 %), ChCl (Fe solvoleaching = 1.6 %) or NH_4Cl (Fe solvoleaching = 15.7 %).

4.3.2. Aqueous leaching of FeS

The leaching of FeS in aqueous systems is rather simpler compared to solvoleaching (Fig. 3). The leaching efficiencies for iron in various aqueous systems were as follows: 86.6 % with 2.0 M HCl, 71.6 % (83.7 % Mn leaching) with 2.0 M H_2SO_4 with 7.5 g/L MnO_2 as the oxidant, 30.0 % with 7.5 g/L $FeCl_3$ in H_2O, and 5.7 % with 2.0 M ChCl. No precipitation was observed from the resulting leach solutions, which is attributed to water's ability to dissolve Fe^{2+} species. H_2S formation was observed in almost all the leaching systems. In the $H_2SO_4 + MnO_2$ system, the H_2S formation was formed initially, as MnO_2 accelerates the kinetics of H_2S oxidation to S^0 (Eq. (19)). In the aqueous $FeCl_3$ leaching system, a red residue was observed, which is likely Fe(III)-oxide/hydroxide. This red residue was formed from the Fe^{3+} species in $FeCl_3$ system, which was precipitated in slightly acidic to neutral conditions (**Fig. S3**).

4.4. Zinc sulfide dissolution (ZnS)

4.4.1. Solvoleaching of ZnS

The solvoleaching results for Zn from ZnS across various solvoleaching ssytems are shown in Fig. 4. Notably, Zn solvoleaching achieved higher efficiency compared to other metals. Specifically, the Zn solvoleaching in the system of D2EHPA + MnO_2 + H_2O reached 58.0 % (with 66.8 % Mn solvoleaching), and H_2S was detected. In particular, H_2S formation might be explained by multistep oxidation reactions. The first step is the reaction between ZnS and H^+ from D2EHPA (Niederkorn, 1985), as ascribed by Eq. (21); this might occur due to the native property of Zn^{2+} (a stronger Lewis acid, compared to Cu^{2+} or Ni^{2+}, for instance (Tapiador et al., 2023)) to allow the Case 4.2 in **Fig. S4** (Strong acid leaching) to happen. Subsequently, H_2S is oxidized to S^0 by MnO_2 (Eq. (20)). The same mechanism might also happen during aqueous leaching of ZnS using H_2SO_4 with MnO_2 as oxidant; however, H_2S formation occurred only during initial time of the aqueous leaching (1 h) due to the more advanced oxidizing activity of MnO_2.

Solvoleaching of ZnS with $H^+_{(org)}$ (from D2EHPA) and MnO_2:

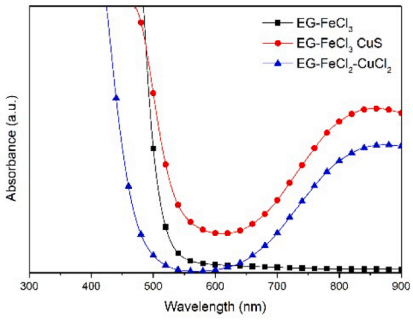

(e)

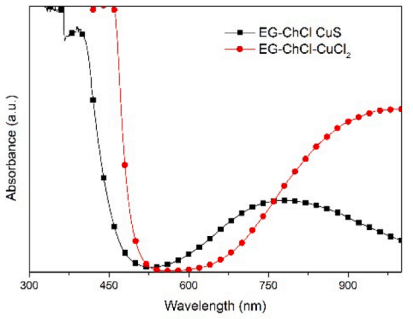

(f)

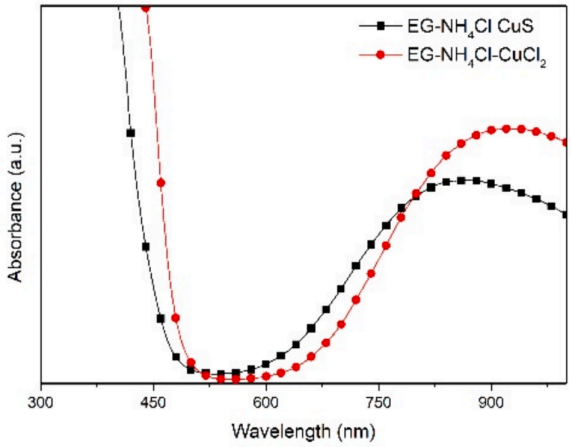

(g)

Fig. 6. (*continued*).

$$ZnS+2H^{+}_{(org)} \rightarrow Zn^{2+} + H_2S_{(g)} \quad (21)$$

In the amoniacal solvoleaching system, Zn solvoleaching was limited to only 15.2 %, with no detectable H_2S formation. This rather limited Zn solvoleaching can be attributed to the high stability of Zn-ammine complexes (**Fig. S4**), which decreases the tendency of Zn^{2+} to be extracted into LIX 84-I. Consequently, this hinders the continuous solvoleaching process.

In all chloride-containing systems, H_2S formation was consistently observed. This can be attributed to the interaction between Zn^{2+} and Cl^{-}, which likely contributes to the formation of a strong acid environment (Peters, 1976). Quantitative dissolution of zinc was attained during the solvoleaching using TBP-HCl and EG-HCl systems. Specifically, a small volume of aqueous solution separated from the TBP-HCl system when storing, but manual shaking could ensure the mixing of the two solutions. This can be attributed by the chemistry properties of Zn^{2+} (**Table S2**).

Interestingly no distinguished phase formation has occurred to the resulting leach solution obtained from the EG-HCl system, thus showing a single-phase solution. The negligible Zn solvoleaching in EG-ChCl system aligns with the Eh-pH diagram (**Fig. S4**), which indicates a wide stability range for ZnS under reductive conditions. When storing the leach solution at room temperature for 24 h, white precipitates were observed. These precipitates are likely due to the low solubility of metals/metal salts in EG at low temperature (Withhead et al., 2010).

The solvoleaching efficiency of Zn in EG-$FeCl_3$ and EG-NH_4Cl was found to be 25.0 % and 21.3 %, respectively, but gray and white precipitates were observed from respective leach solutions. This had not happened from the resulting solutions of $ZnCl_2$ salt dissolved into EG or EG-NH_4Cl. Therefore, it is proposed that the precipitations happened due to the difference in chemistry of Zn^{2+} and Fe^{2+}, and more specifically the low solubility of Fe^{2+} in EG (as the Fe^{2+} formed by oxidizing ZnS in the EG-$FeCl_3$ system); this could refer to the HSAB theory and hydration properties of the metal ions in **Table S2**, besides the effect of cooling (room temperature) and the presence of sulfur-containing anions in the solution from EG-NH_4Cl system.

4.4.2. Aqueous leaching of ZnS

The Zn leaching in H_2SO_4-MnO_2 system could reach almost quantitative, along with 89.0 % Mn leaching (Fig. 4). The leaching of ZnS was almost similar to other aqueous leaching systems (HCl, H_2O-$FeCl_3$, H_2O-ChCl) compared to those in solvoleaching systems. The tendency toward H_2S formation was also observed in the evaluated aqueous leaching systems (Table 1(b)).

4.5. Solvoleaching of lead sulfide (PbS)

About 30.9 % of lead (along with 61.3 % of manganese) were extracted in the D2EHPA+MnO_2 + H_2O system (Table 3). Only a small part of the lead acetate paper turned black, which was probably due to the same reason as observed for ZnS relating to the interaction between PbS and H^{+} to form H_2S (in accordance with the Case 5.2 in **Fig. S5**). However, Pb^{2+} being a relatively soft Lewis acid (Kerner et al., 2019), results in lower acidity in the solvent system compared to Zn^{2+}, and consequently, generate less H_2S.

The solvoleaching efficiency of Pb using the ammoniacal solvoleaching reached only 16.5 % (Table 3). The limited Pb solvoleaching in ammoniacal system agreed to that reported by Golomeov et al. (2003). Unlike copper/nickel/iron/zinc, lead hardly forms ammine complexes (**Fig. S5**), but the addition of H_2O_2 into the system could oxidize PbS to $PbSO_4$ or PbO (Cârstea et al., 2023), which may be responsible for the solvoleaching.

The instant precipitation of $PbCl_2$ was observed during solvoleaching with TBP-HCl, with minimal loading in TBP. This agreed to the result when $PbCl_2$ salt was dissolved in TBP (**Table S1**). H_2S formation was

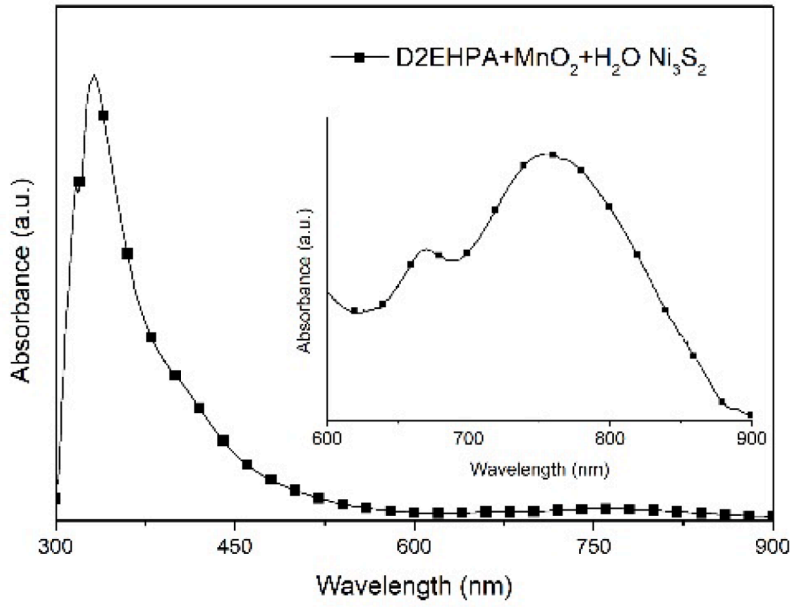

(a)

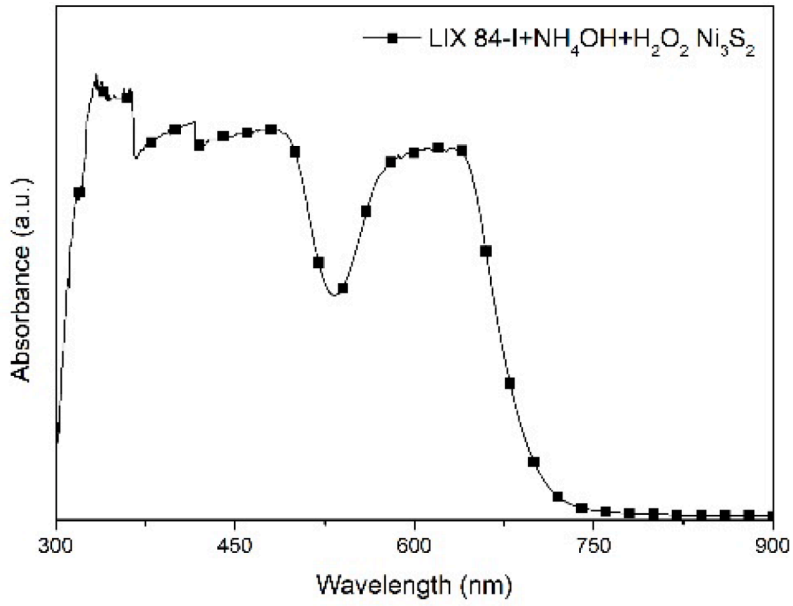

(b)

Fig. 7. UV–Vis spectra of Ni-containing solutions from the solvoleaching systems: (a) D2EHPA + MnO_2, (b) LIX 84-I + NH_4OH + H_2O_2, (c) TBP-HCl, (d) EG-HCl, (e) EG-$FeCl_3$, (f) EG-ChCl and (d) EG-NH_4Cl.

observed in accordance with Case 5.2 (Fig. S5). A similar case was observed in the EG-HCl system, where only 15.8 % of the leached Pb loaded into TBP, while the majority of the leached Pb formed $PbCl_2$ precipitates (Table 3); similar was observed when $PbCl_2$ salt was dissolved in EG. Fewer precipitates were formed during the solvoleaching for PbS using EG-ChCl, EG-NH_4Cl and EG-$FeCl_3$ since less chloride was

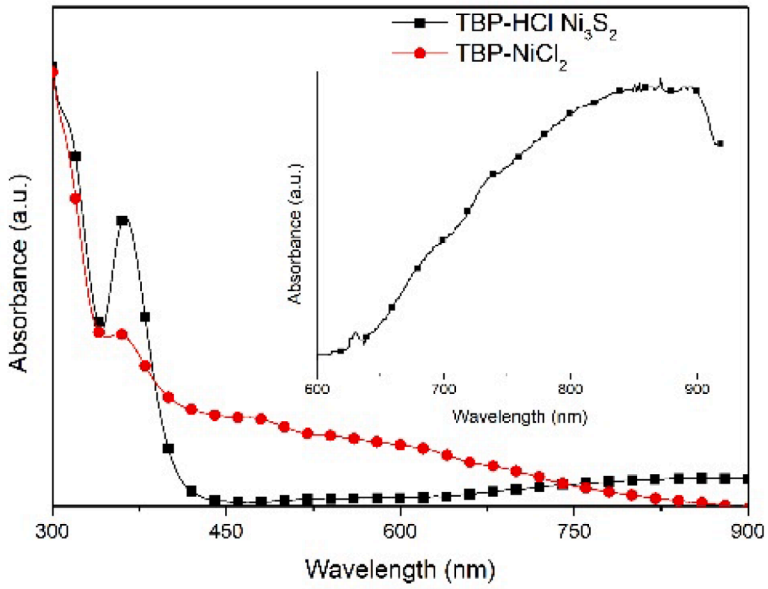

(c)

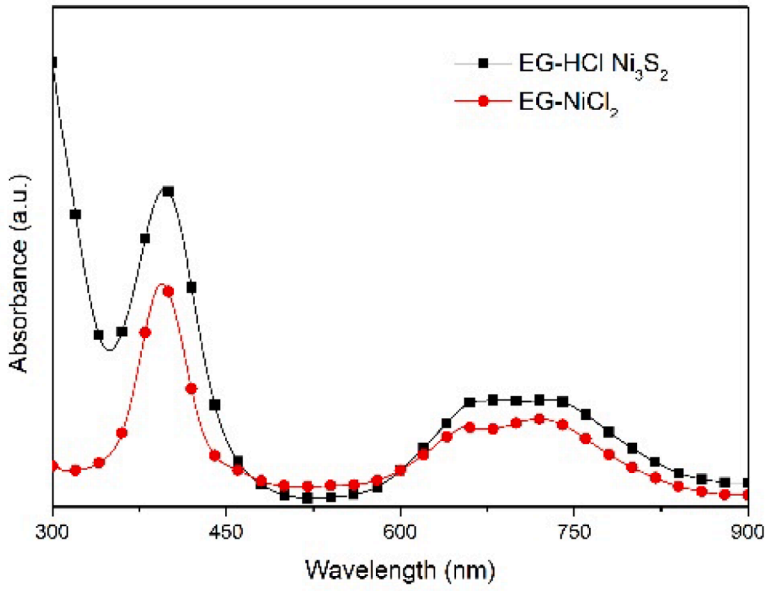

(d)

Fig. 7. (*continued*).

available in these systems. Black precipitates from EG-ChCl and EG-NH_4Cl were observed likely because of the formation of intermediate sulfur-containing compounds in the reductive (EG-ChCl) and alkaline (EG-NH_4Cl) systems. Meanwhile, chemistry between Fe^{2+}-Pb^{2+} in EG could also explain the gray precipitates formed from the EG-$FeCl_3$ solution.

4.6. Solvoleaching of molybdenum sulfide (MoS_2)

Among all the metal sulfides investigated, molybdenum disulfide (MoS_2) did not exhibit any dissolution in the studied solvoleaching systems. Possible reasons include: (i) the solvents may lack sufficient strength to dissolve Mo species, or (ii) the inherent stability of MoS_2. To address the first reason, the solvoleaching of another molybdenum

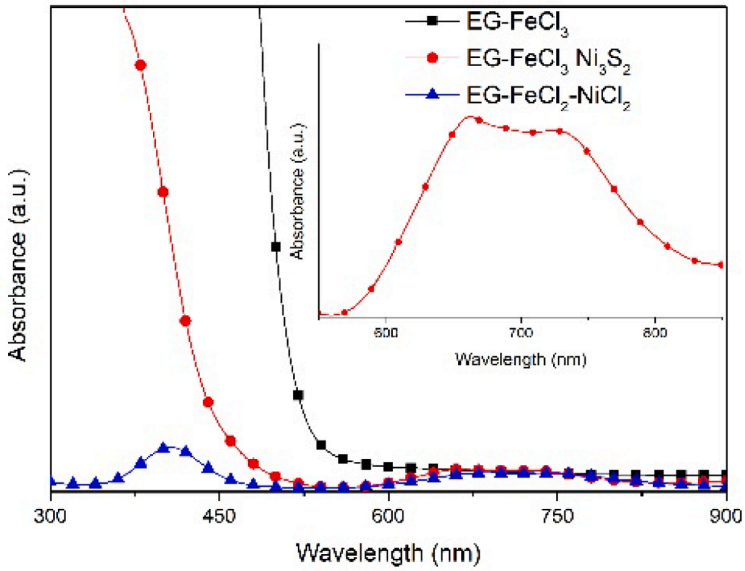

(e)

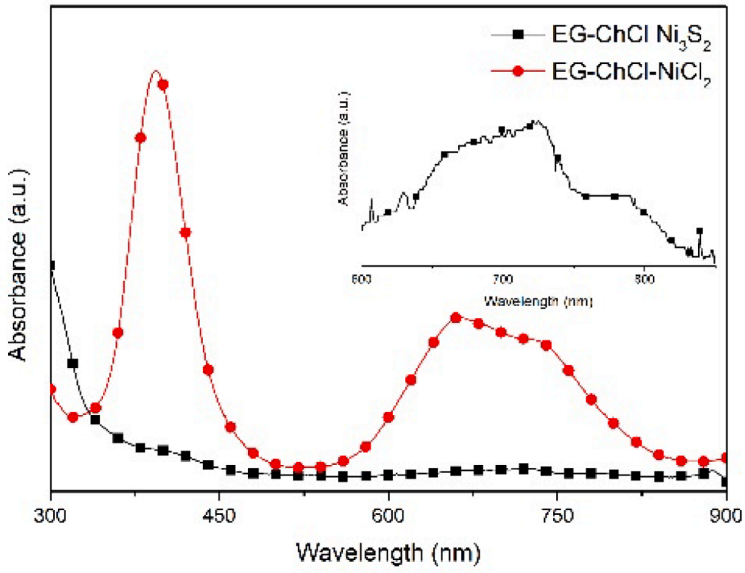

(f)

Fig. 7. (*continued*).

compound, MoO_2, was examined in several solvoleaching systems: ammoniacal solvoleaching, EG-ChCl, EG-HCl and EG-NH_4Cl. The solvoleaching of MoO_2 was carried out under the same conditions as that of MoS_2. The results, as shown in Table 3, indicate that MoO_2 could be leached to the extent of 29.0 % in ammoniacal solvoleaching, 18.1 % in EG ChCl, and 46.2 % in EG-HCl, but only 0.2 % in EG-NH_4Cl. Such solvoleaching of MoO_2 in EG-ChCl can be understood from its reductive property, which enables it to bring the metal into soluble species (Zeng and Cheng, 2009). The higher solvoleaching of MoO_2 in EG-HCl is attributed to the capability of HCl to break the lattice of MoO_2.

The results of the solvoleaching of MoO_2 also indicate that the negligible solvoleaching of MoS_2 in the investigated solvent systems is attributed to the second reason: the high stability of MoS_2. This is evidenced by the Eh-pH diagram for the Mo-S-H_2O system (**Fig. S6**), which shows that MoS_2 remains stable under the conditions studied. Indeed, the challenges in leaching MoS_2 have been documented in the literature

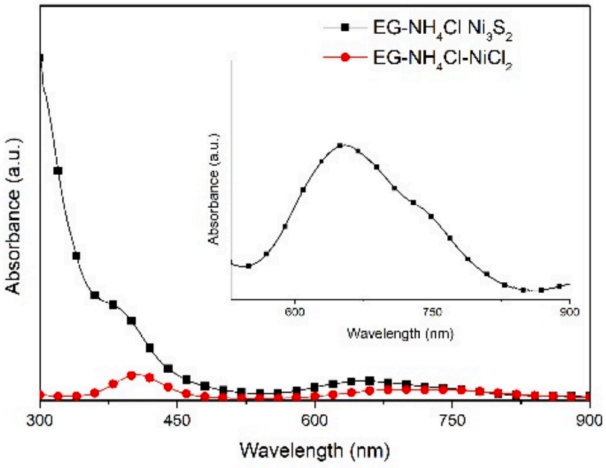

(g)

Fig. 7. (*continued*).

(Peeters, 1976). The formation of ionic hydroxo and oxide molybdenum can occur in slightly acidic and alkaline solutions, but the investigated solvents in the present study do not subscribe to that category.

5. Analysis of leach solutions

The obtained leach solutions were analyzed via FTIR and UV–Vis, as follows.

5.1. FTIR results

- **D2EHPA system**

The active groups of D2EHPA, P—O–H, P═O and O–H, are shown at bands 1018, 1224 and 1605–1868 cm^{-1} (Darvishi et al., 2005), respectively, as shown in Fig. 5(a). The bands underwent vibration and reduced intensities as a result of solvoleaching, proving their participation in the metal-D2EHPA complexation. No discernible occurrences were shown in the spectra of each Cu/Ni/Zn-D2EHPA, suggesting that the metal ions underwent the same complexation mechanism. The sole distinction was noted in the Fe-loaded D2EHPA, where an O–H adsorption-induced band shift from 1224 to 1221 cm^{-1} was observed (Huei et al., 2016). This further substantiated the aforementioned account regarding the importance of incorporating H_2O as the catalyst in the solvoleaching process of iron.

- **LIX 84-I system**

The broad absorption band observed at 3253–3565 cm^{-1}, as shown in Fig. 5(b), corresponds to the active group of LIX 84-I, N—O–H group (de Gyves et al., 2006). It was anticipated that the prominence of this band diminished following solvoleaching (metal-LIX 84-I complexation). The presence of ammonia in the loaded LIX 84-I was confirmed by the formation of a new peak at 966 cm^{-1} and the observation of decreasing intensities at 1026 cm^{-1} (Alguacil et al., 2001; Tang et al., 2016). These results provide further support for the previous discussion regarding the equilibration of ammonia onto LIX 84-I after certain time of solvoleaching.

- **TBP system**

Significant disparities were identified when comparing the spectra of original TBP and metal-loaded TBP (Fig. 5(c)). The presence of vibrations within the range of 2514–2816 cm^{-1} in metal-loaded TBP may be ascribed to the generation of [TBP•metal chloride] complexes or remaining [TBP•HCl] (Yi et al., 2020). The shifted peaks at 1279 cm^{-1} (for P═O stretching) to 1220 cm^{-1} and 1026/973 cm^{-1} (for P—O—C) to 1018/1007 cm^{-1} also assigned for the same reason (Su et al., 2020; Yi et al., 2020). The decreased intensities at 732 and 809 cm^{-1} further suggested the existence of remaining equilibrated HCl (Zuo et al., 2019). In the meantime, the Cu- and Ni-chloride-TBP spectra were identical.

- **EG system**

The FTIR spectra of EG and the leach solutions obtained from solvoleaching metal sulfides with EG-HCl, EG-$FeCl_3$, EG-ChCl and EG-NH_4Cl are illustrated in Fig. 5**(d–g)**), respectively. The absorption band of EG at 3300 cm^{-1} (assigned for —OH) shifted to lower wavenumber in the spectra of leach solutions of EG-HCl, indicating a strong involvement of the group (—OH) in the dissolution of HCl in EG (Tran and Hang, 2018). This band also underwent a change of intensity in the EG-ChCl spectra, which can be attributed to the hydrogen bonding that takes place between EG and ChCl (Tran and Hang, 2018). This did not happen to EG-$FeCl_3$ and EG-NH_4Cl, probably due to the lower hydrogen bonding capacity of these latter active components. However, the chloride characteristics were indicated by the increases in the peaks of group frequencies of EG at 2357/2354 cm^{-1} and 1629–1700 cm^{-1} (assigned for C—O vibrational stretching (Netala et al., 2018; Vatanpour et al., 2020). The peaks of these group frequencies exhibited a further increase subsequent to the solvoleaching process. No discernible differences were found in the spectra of each metal, with the exception of varying peak intensities that correspond to the results of solvoleaching, suggesting that the dissolution of the metals in EG was facilitated by the same mechanism.

5.2. Uv–vis results

The leach solutions obtained from the solvoleaching of CuS, Ni_3S_2 and FeS were analyzed via UV–Vis analysis. As a comparison, the solutions produced by dissolving corresponding chloride salts ($CuCl_2$, $NiCl_2$, $FeCl_3$ and $FeCl_2$) were also analyzed. Solutions from the solvoleaching of other sulfides were excluded due to either their transparency or direct precipitation.

- **Cu-containing solutions**

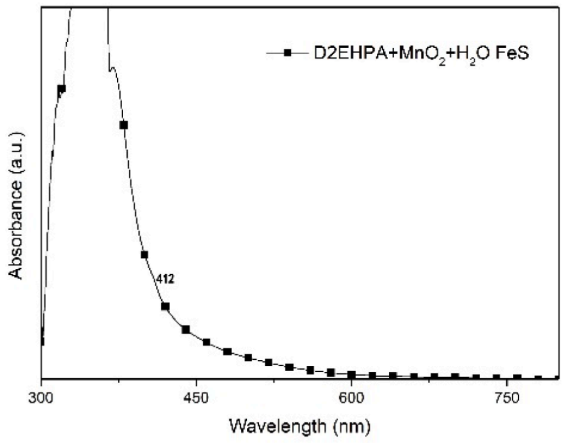

(a)

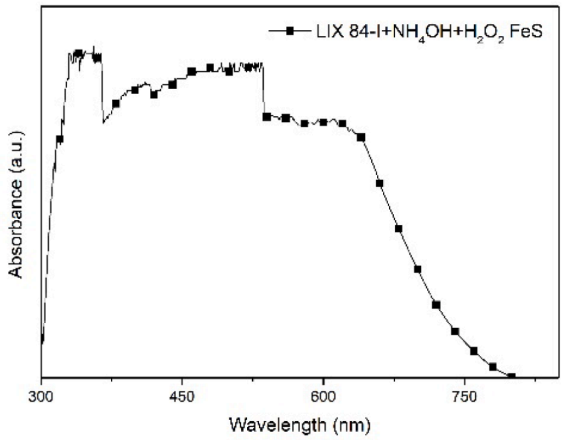

(b)

Fig. 8. UV–Vis spectra of Fe-containing solutions from the solvoleaching systems: (a) D2EHPA + MnO_2, (b) LIX 84-I + NH_4OH + H_2O_2, (c) TBP-HCl, (d) EG-HCl, (e) EG-$FeCl_3$, (f) EG-ChCl and (d) EG-NH_4Cl.

The UV–Vis spectra of the leach solutions from the CuS solvoleaching revealed the presence of Cu^{2+} ions (Fig. 6). As depicted in Fig. 6(a), the broad band that peaked at 800 nm indicated the presence of Cu^{2+} in the loaded D2EHPA (Peeters et al., 2022; Van de Voorde et al., 2005), as shown in Fig. 6(a). The clearly visible absorption peak at 340 nm in this spectra is indicative of an electron transfer taking place during the solvoleaching process. The coordination between Cu^{2+} and nitrogen atom from oxime groups was indicated by the absorption peak at band 589–703 nm in the loaded LIX 84-I spectra (Fig. 6(b)) (Guo et al., 2021). The spectra of loaded TBP and EG systems also exhibited the broad absorption peaks of Cu^{2+} (Fig. 6**(c–g)**); these spectra were all similar to those obtained when $CuCl_2$ salt was dissolved in the solutions. Shifting peaks were due to the differences of chloride presences in the real leach solutions and those from the dissolution of $CuCl_2$ salt.

- **Ni-containing solutions**

The spectra of loaded D2EHPA revealed the presence of octahedral coordination of Ni(II) (Fig. 7(a)). This particular coordination scheme enables the occurrence of three spin-allowed transition stages, from the ground state $^3A_{2g}(F)$, to the states $^3T_{2g}(F)$, $^3T_{1g}(F)$ and $^3T_{1g}(P)$. The peak at 412 nm in Fig. 7(a) represents the transition $^3A_{2g}(F) \rightarrow {}^3T_{1g}(P)$, and the peak at 755 nm accompanied by a shoulder at 670 nm signifies the transition $^3A_{2g}(F) \rightarrow {}^3T_{1g}(F)$. The third transition ($^3A_{2g}(F) \rightarrow {}^3T_{2g}(F)$) fell outside the assessed spectral range. Electron transfer continued to be indicated by the conspicuous absorption peak at 335 nm. The presence of an absorption peak at 614 nm in Fig. 7(b) suggests the coordination between Ni^{2+} and N-atom from oxime group (Feng et al., 2011; Guo et al., 2021). The UV–Vis spectra of nickel-containing TBP and EG solutions (Fig. 7**(c–g)**) could be elucidated using the same descriptions as D2EHPA; shifts were observed relative to D2EHPA, which were influenced by the presence of chloride or Fe^{2+} (in the case of leach solution from the EG-$FeCl_3$ system).

- **Fe-containing solutions**

As mentioned previously, iron was extracted onto D2EHPA as Fe^{3+}/$Fe(OH)^{2+}$, in contrast to other metals. The characteristic peak of Fe^{3+}

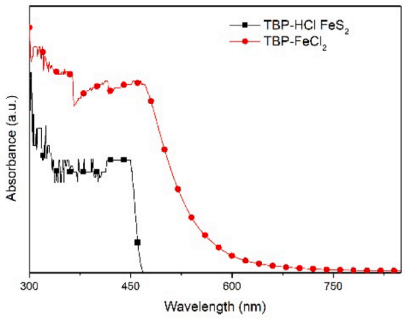

(c)

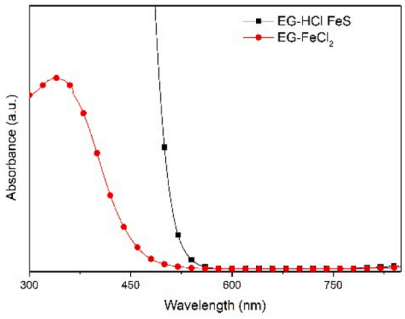

(d)

Fig. 8. (*continued*).

was observed at 412 nm (Fig. 8(a)), providing further evidence for this (Giordano et al., 2012). The UV–Vis spectra of Fe-LIX 84-I (Fig. 8(b)) exhibit two distinct peaks at 494 and 615 nm. These peaks correspond to the electron transfer and the transition $^{6}A_{1g} \rightarrow {}^{4}T_{2g}(D)$ (El-Saied et al., 2018); this spectra agreed well to that reported by Alattar et al. (2020), which confirmed the existence of Fe^{3+}-N atom complex. A similarity was observed in the spectra of the TBP and EG-based leach solutions and those obtained by dissolving $FeCl_2$ salt (Fig. 8(c–g)), suggesting the existence of Fe^{2+} in the solutions.

6. Limitations in solvoleaching studies

The findings presented above reveal intriguing phenomena and suggest that the solvoleaching process holds promise as an effective method for treating metal sulfides. However, several limitations have been identified. A notable limitation of this study is the reliance on small-scale experiments, a common issue observed in other solvoleaching studies (Li et al., 2020; Carlesi et al., 2022; Palden et al., 2019; Peeters et al., 2022). The small scale of experiments presents challenges, particularly in analyzing residues from solvoleaching and any resulting precipitates. Additionally, the limited scale impedes the ability to obtain sufficient leach solutions for metal recovery experiments and complicates the investigation of solvent recyclability.

Another limitation observed from the findings is the apparent low selectivity of the investigated solvoleaching systems, although it was not specifically examined in the present study. This is particularly evident when considering the solvoleaching behavior of Cu, Ni, and Zn, as their solvoleaching results were comparable. This presents challenges when treating actual materials (sulfide minerals/composites). Enhancing selectivity may be achieved through methods such as selective stripping or the application of different solvoleaching systems; however, these approaches are beyond the scope of the current study.

Furthermore, the findings suggest that the dissolution of certain metals, such as iron, necessitates the presence of water or aqueous lixiviants. Hence, the complete elimination of water from the process is not feasible. While water may evaporate during the process, especially at elevated temperatures like 90 °C (as used in this study), it necessitates attention to the consequent pressure rise when designing the reactor for solvoleaching.

Viscosity presents an additional challenge in the context of solvoleaching investigations. The present study utilized a temperature of 90 °C, with the exception of ammoniacal solvoleaching at 25 °C, in order to address the problem of viscosity. However, it was worth noting that when the leach solutions were cooled to room temperature, there was a significant increase in viscosity. This led to increased challenges in the treatment of leach solutions.

7. Conclusions

This study examines the applicability of solvoleaching for treating metal sulfides (CuS, Ni_3S_2, FeS, ZnS, PbS, MoS_2) across a range of solvoleaching systems (D2EHPA + MnO_2 + H_2O, ammoniacal solvoleaching, TBP-HCl and EG with each of HCl/ChCl/NH_4Cl/$FeCl_3$. The results demonstrate that solvoleaching has potential for treating CuS, Ni_3S_2, FeS, ZnS and PbS, except MoS_2. The solvoleaching behaviors were dependent on the following aspects: (i) the inherent characteristics of the metals being targeted, including their sulfide compounds and ions, (ii) the solvating properties of the solvents with respect to the specific metal ions or complexes; and (iii) the presence or nature of active components, like oxidants, acids, Cl source, etc. Thermodynamic tools, such as Eh-pH diagrams, Gibbs free energy change and solvation properties of the metal ions, as well as the hard and soft acid-base (HSAB) theory, were employed to predict and elucidate the solvoleaching results. The following conclusions are drawn from the solvoleaching results pertaining to the targeted metal sulfides:

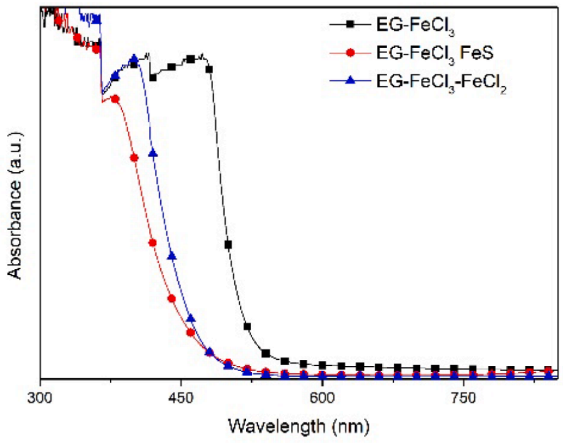

(e)

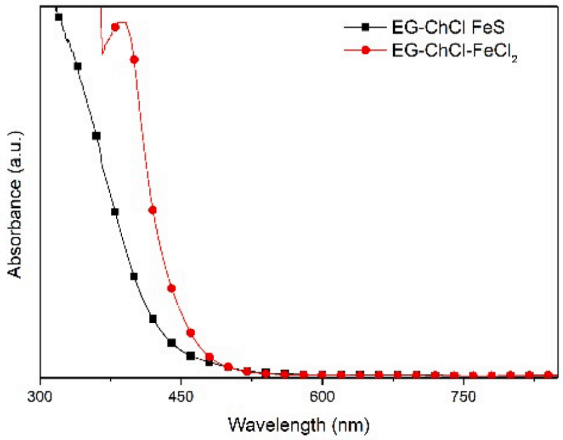

(f)

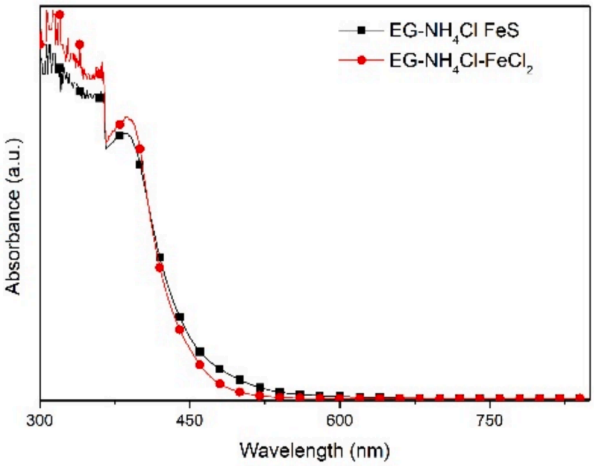

(g)

Fig. 8. (*continued*).

- Cu solvoleaching from CuS could reach almost quantitative in TBP-HCl and EG-HCl; it was below 50 % in other solvoleaching systems, and it noted the lowest efficiency (14.1 %) in EG-ChCl. Minor issues were found, such as the formation of a small amount of separated aqueous solution in the HCl-equilibrated TBP system and the precipitation of $Cu(NH_3)_x(Cl/SO_4)y$ salts in the EG-NH_4Cl system at room temperature. These issues were attributed to Cu^{2+} being a borderline Lewis acid and its solvation properties in the solvents/extractants.
- Ni solvoleaching could also reach almost quantitative in TBP-HCl and EG-HCl, and it was much lower in other solvoleaching systems compared to that of copper. A higher volume of separated aqueous solution in TBP-HCl leach solution was observed. Such results were due to Ni^{2+} having a higher hydrophilicity.
- Generally, Fe solvoleaching was lower than that of Cu and Ni, with the maximum Fe solvoleaching attained being 86.6 % in EG-HCl system. This was due to low coordination between Fe^{2+} and the extractants/solvents, which also leading to the formation of numerous precipitates. In particular, incorporating H_2O and MnO_2 in the D2EHPA system and H_2O_2 in the ammoniacal solvoleaching system helped oxidize Fe^{2+} to Fe^{3+}/$FeOH^{2+}$ to advance Fe solvoleaching.
- Zn solvoleaching from ZnS generally had better yields compared to other metals while reaching almost quantitative in TBP-HCl (lesser separated aqueous solution) and EG-HCl. Exception was the lower Zn solvoleaching in ammoniacal solvoleaching (15.2 %) compared to that of Cu due to higher stability of Zn-ammine complexes. The formation of H_2S was observed in all solvoleaching systems.
- PbS treatment with Cl-containing solvents led to precipitation due to the stability of $PbCl_2$, resulting in low solvation in the solvents.
- Solvoleaching of Mo from MoS_2 showed negligible results in all solvent systems due to the sulfide's high stability.

Some limitations were highlighted, including: the use of small-scale experiments, low selectivity, the need for water and high viscosity. To address these limitations, further investigation is required to comprehensively examine the process of solvoleaching metal sulfides. This includes conducting comprehensive analysis of residues and evaluating the quality of precipitates (if any). Future studies should also investigate the solvoleaching of mixed metal sulfides and real sulfide minerals to assess selectivity, kinetics, and scalability of the process while also optimizing the solvoleaching process by investigating the effect of solvoleaching parameters. Additionally, the stripping behavior, particularly when using water-immiscible solvents such as D2EHPA, TBP, or LIX 84-I dissolved in kerosene, and recyclability of the organic solvents (a key point of sustainability of solvoleaching process) should be examined in detail to enhance selectivity and process efficiency.

CRediT authorship contribution statement

Kurniawan Kurniawan: Writing – original draft, Methodology, Investigation, Formal analysis, Data curation, Conceptualization. **Sookyung Kim:** Supervision, Project administration, Funding acquisition. **Mooki Bae:** Formal analysis. **Alexandre Chagnes:** Writing – review & editing. **Jae-chun Lee:** Writing – review & editing, Supervision.

Declaration of competing interest

The authors declare that they have no known competing financial interests or personal relationships that could have appeared to influence the work reported in this paper.

Data availability

Data will be made available on request.

Acknowledgement

This work was supported by the National Research Foundation of Korea (NRF) grant funded by the Korea government (MSIT) (RS-2023-00254424) and supported by the Korea Institute of Energy Technology Evaluation and Planning (KETEP) grant funded by the Korea government (MOTIE) (20229A10100070, Development of Pt catalysts precursor with low carbon emission recycling process from waste PEMFC).

Appendix A. Supplementary data

Supplementary data to this article can be found online at https://doi.org/10.1016/j.mineng.2024.109005.

References

Alattar, R. A., Hassan, Z. M., Abass, S. K., & Ahmad, L. M. (2020, December). Synthesis, characterization and study the photodecolorization of Schiff base Fe (III) complex in ZnO/Uv-A light system. In *AIP Conference Proceedings* (Vol. 2290, No. 1). AIP Publishing.

Alguacil, F.J., Alonso, M., Lopez, F.A., 2001. Influence of ammonium salts on solvent extraction of nickel using LIX 54. J. Chem. Eng. Jpn. 34 (1), 83–86.

Anggara, S., Bevan, F., Harris, R.C., Hartley, J.M., Frisch, G., Jenkin, G.R., Abbott, A.P., 2019. Direct extraction of copper from copper sulfide minerals using deep eutectic solvents. Green Chem. 21 (23), 6502–6512.

Binnemans, K., Jones, P.T., 2017. Solvometallurgy: an emerging branch of extractive metallurgy. Journal of Sustainable Metallurgy 3, 570–600.

Carlesi, C., Harris, R.C., Abbott, A.P., Jenkin, G.R., 2022. Chemical dissolution of chalcopyrite concentrate in choline chloride ethylene glycol deep eutectic solvent. Minerals 12 (1), 65.

Cârstea, C.E., Sandu, A.M., Duinea, M.I., Dăbuleanu, I., Chiriță, P., 2023. Aqueous oxidation of galena by hydrogen peroxide in hydrochloric acid. Can. Metall. Q. 1–10.

Chaerun, S.K., Winarko, R., Yushandiana, F., 2023. Biohydrometallurgy: paving the way for a greener future of mineral processing in Indonesia-A mini review. Current Research on Biosciences and Biotechnology 5 (1), 299–307.

Crundwell, F., Moats, M., Ramachandran, V., 2011. Extractive metallurgy of nickel, cobalt and platinum group metals. Elsevier.

Darvishi, D., Haghshenas, D.F., Alamdari, E.K., Sadrnezhaad, S.K., Halali, M., 2005. Synergistic effect of Cyanex 272 and Cyanex 302 on separation of cobalt and nickel by D2EHPA. Hydrometall. 77 (3–4), 227–238.

de Gyves, J., Hernández-Andaluz, A. M., & de San Miguel, E. R. (2006). LIX®-loaded polymer inclusion membrane for copper (II) transport: 2. Optimization of the efficiency factors (permeability, selectivity, and stability) for LIX® 84-I. *Journal of Membrane Science*, *268*(2), 142-149.

Devi, N., 2015. Extraction of manganese (II) from acidic buffer medium using D2EHPA and Cyanex 272 as extractants. J. Chem. Pharm. Res 7 (4), 766–776.

El-Saied, F.A., Salem, T.A., Shakdofa, M.M., Al-Hakimi, A.N., Radwan, A.S., 2018. Antitumor activity of synthesized and characterized Cu (II), Ni (II) and Co (II) complexes of hydrazone-oxime ligands derived from 3-(hydroxyimino) butan-2-one. Beni-Suef University Journal of Basic and Applied Sciences 7 (4), 420–429.

Faris, N., Powenceby, M.I., Bruckard, W.J., Chen, M., 2023. The direct leaching of nickel sulfide flotation Concentrates–a historic and state-of-the-art review part I: Piloted processes and commercial operations. Miner. Process. Extr. Metall. Rev. 44 (6), 407–435.

Feng, L., Zhang, Y., Wen, L., Chen, L., Shen, Z., Guan, Y., 2011. Colorimetric filtrations of metal chelate precipitations for the quantitative determination of nickel (II) and lead (II). Analyst 136 (20), 4197–4203.

Giordano, D., Boron, I., Abbruzzetti, S., Van Leuven, W., Nicoletti, F.P., Forti, F., Bruno, S., Cheng, C.C., Moens, L., di Prisco, G., Verde, C., 2012. Biophysical characterisation of neuroglobin of the icefish, a natural knockout for hemoglobin and myoglobin. Comparison with Human Neuroglobin. *Plos One* 7 (12), e44508.

Golomeov, B., Krstev, B., & Krstev, A. (2003). Processing of galena synthetic mixures for producing lead and elemental sulfur. www.ugd.edu.mk.

Guo, S.Z., Wang, J.F., Feng, S.S., Zhao, L., 2021. Co (II) and Ni (II) bis (salamo)-based tetraoxime complexes: Syntheses, structural characterizations, fluorescence properties, and Hirshfeld analyses. J. Coord. Chem. 74 (7), 1181–1195.

Gutmann, V., 1968. Principles of Coordination Chemistry in Non-Aqueous Solutions. In: Coordination Chemistry in Non-Aqueous Solutions. Springer Vienna, Vienna, pp. 12–34.

Huei, G.O.S., Muniyandy, S., Sathasivam, T., Veeramachineni, A.K., Janarthanan, P., 2016. Iron cross-linked carboxymethyl cellulose–gelatin complex coacervate beads for sustained drug delivery. Chem. Pap. 70 (2), 243–252.

Ineza, C., Pearce, B.H., Begum, N.M., Luckay, R., 2022. The synthesis and use of new amic acid extractants for the selective extraction of Cu (II), Ni (II) and Co (II) from other base metal ions in acidic medium. Sep. Sci. Technol. 57 (1), 13–27.

Kerner, R. A., Schloemer, T. H., Schulz, P., Berry, J. J., Schwartz, J., Sellinger, A., & Rand, B. P. (2019). Amine additive reactions induced by the soft Lewis acidity of Pb 2+ in halide perovskites. Part I: evidence for Pb–alkylamide formation. *Journal of Materials Chemistry C*, *7*(18), 5251-5259.

Kurniawan, K., & Mubarok, M. Z. (2018, April). Dissolution behavior of Cu, Fe and Zn from gold sulfide concentrate during pre-oxidation using ozone in neutral media. In *AIP Conference Proceedings* (Vol. 1945, No. 1). AIP Publishing.

Kadivar, S., Akbari, H., Vahidi, E., 2024. Environmental footprint of gold production: a focus on sulfide mineral processing. Clean Technologies and Environmental Policy 1–15.

Li, X., Binnemans, K., 2021. Oxidative dissolution of metals in organic solvents. Chem. Rev. 121 (8), 4506–4530.

Li, Z., Li, X., Raiguel, S., Binnemans, K., 2018. Separation of transition metals from rare earths by non-aqueous solvent extraction from ethylene glycol solutions using Aliquat 336. Sep. Purif. Technol. 201, 318–326.

Li, X., Monnens, W., Li, Z., Fransaer, J., Binnemans, K., 2020. Solvometallurgical process for extraction of copper from chalcopyrite and other sulfidic ore minerals. Green Chem. 22 (2), 417–426.

Marcus, Y., 1991. Thermodynamics of solvation of ions. Part 5. —Gibbs free energy of hydration at 298.15 K. J. Chem. Soc. Faraday Trans. 87 (18), 2995–2999.

Mubarok, M.Z., Winarko, R., Chaerun, S.K., Rizki, I.N., Ichlas, Z.T., 2017. Improving gold recovery from refractory gold ores through biooxidation using iron-sulfur-oxidizing/sulfur-oxidizing mixotrophic bacteria. Hydrometall. 168, 69–75.

Mubarok, M.Z., Sukamto, K., Ichlas, Z.T., Sugiarto, A.T., 2018. Direct sulfuric acid leaching of zinc sulfide concentrate using ozone as oxidant under atmospheric pressure. Miner. Metall. Process 35, 133–140.

Nakagawa, S., Nishimura, H., Kodera, F., 2018. Detection of Chlorine in a Non-aqueous Solution via Anodic Oxidation and a Photochemical Reaction. Anal. Sci. 34 (1), 1–4.

Nayak, A., Jena, M.S., Mandre, N.R., 2022. Beneficiation of lead-zinc ores–a review. Miner. Process. Extr. Metall. Rev. 43 (5), 564–583.

Netala, V. R., Bukke, S., Domdi, L., Soneya, S., G. Reddy, S., Bethu, M. S., Kotakdi, V. S., Saritha, K. V., & Tartte, V. (2018). Biogenesis of silver nanoparticles using leaf extract of Indigofera hirsuta L. and their potential biomedical applications (3-in-1 system). *Artificial Cells, Nanomedicine, and Biotechnology*, *46*(sup1), 1138-1148.

Nguyen, V.N.H., Song, S.J., Lee, M.S., 2022. Effect of Ethylene Glycol on the dissolution of Palladium with HCl solution containing oxidizing agents and selective precipitation of Pd (IV) compound. Korean Journal of Metals and Materials 60 (7), 502–510.

Nicol, M.J., 2018. A comparative assessment of the application of ammonium chloride and glycine as lixiviants in the heap leaching of chalcopyritic ores. Hydrometall. 175, 285–291.

Niederkorn, J.S., 1985. Kinetic study on catalytic leaching of sphalerite. JOM 37 (7), 53–56.

Palden, T., Regadío, M., Onghena, B., Binnemans, K., 2019. Selective metal recovery from jarosite residue by leaching with acid-equilibrated ionic liquids and precipitation-stripping. ACS Sustain. Chem. Eng. 7 (4), 4239–4246.

Panda, S., Akcil, A., Pradhan, N., Deveci, H., 2015. Current scenario of chalcopyrite bioleaching: a review on the recent advances to its heap-leach technology. Bioresour. Technol. 196, 694–706.

Peeters, N., Janssens, K., de Vos, D., Binnemans, K., Riaño, S., 2022. Choline chloride–ethylene glycol based deep-eutectic solvents as lixiviants for cobalt recovery from lithium-ion battery cathode materials: are these solvents really green in high-temperature processes? Green Chem. 24 (17), 6685–6695.

Peters, E., 1976. Direct leaching of sulfides: chemistry and applications. Metallurgical Transaction B 7 (B).

Qin, H., Hu, X., Wang, J., Cheng, H., Chen, L., Qi, Z., 2020. Overview of acidic deep eutectic solvents on synthesis, properties and applications. Green Energy Environ. 5 (1), 8–21.

Schippers, A., Jørgensen, B.B., 2001. Oxidation of pyrite and iron sulfide by manganese dioxide in marine sediments. Geochim. Cosmochim. Acta 65 (6), 915–922.

Su, H., Li, Z., Zhang, J., Zhu, Z., Wang, L., Qi, T., 2020. Recovery of lithium from salt lake brine using a mixed ternary solvent extraction system consisting of TBP, FeCl3 and P507. Hydrometall. 197, 105487.

Tang, F., Li, X., Wei, C., Fan, G., Zhu, R., Li, C., 2016. Synergistic extraction of zinc from ammoniacal/ammonia sulfate solution by a mixture of β-diketone and 2-hydroxy-5-nonylacetophenone oxime. Hydrometall. 162, 42–48.

Tapiador, J., García-Rojas, E., López-Patón, P., Calleja, G., Orcajo, G., Martos, C., Leo, P., 2023. Influence of divalent metal ions on CO2 valorization at room temperature by isostructural MOF-74 materials. J. Environ. Chem. Eng. 11 (2), 109497.

Toro, N., Rodríguez, F., Rojas, A., Robles, P., Ghorbani, Y., 2021. Leaching manganese nodules with iron-reducing agents–A critical review. Miner. Eng. 163, 106748.

Tran, P.H., Hang, A.H.T., 2018. Deep eutectic solvent-catalyzed arylation of benzoxazoles with aromatic aldehydes. RSC Adv. 8 (20), 11127–11133.

Van De Voorde, I., Pinoy, L., Courtijn, E., Verpoort, F., 2005. Influence of acetate ions and the role of the diluents on the extraction of copper (II), nickel (II), cobalt (II), magnesium (II) and iron (II, III) with different types of extractants. Hydrometall. 78 (1–2), 92–106.

Vatanpour, V., Dehqan, A., Harifi-Mood, A.R., 2020. Ethaline deep eutectic solvent as a hydrophilic additive in modification of polyethersulfone membrane for antifouling and separation improvement. J. Membr. Sci. 614, 118528.

Vera, M., Schippers, A., Hedrich, S., Sand, W., 2022. Progress in bioleaching: fundamentals and mechanisms of microbial metal sulfide oxidation–part A. Appl. Microbiol. Biotechnol. 106 (21), 6933–6952.

Watling, H.R., 2006. The bioleaching of sulphide minerals with emphasis on copper sulphides—a review. Hydrometall. 84 (1–2), 81–108.

Withhead, A.H., Polzler, M., Gollas, B., 2010. Zinc electrodeposition from a deep eutectic system containing choline chloride and ethylene glycol. Journal of the Electrochemical Soceity 157 (6), D238.

Yan, B., Krishnamurthy, D., Hendon, C.H., Deshpande, S., Surendranath, Y., Viswanathan, V., 2017. Surface restructuring of nickel sulfide generates optimally coordinated active sites for oxygen reduction catalysis. Joule 1 (3), 600–612.

Yi, X., Huo, G., Tang, W., 2020. Removal of Fe (III) from Ni-Co-Fe chloride solutions using solvent extraction with TBP. Hydrometall. 192, 105265.

Zeng, L., Cheng, C.Y., 2009. A literature review of the recovery of molybdenum and vanadium from spent hydrodesulphurisation catalysts: Part I: Metallurgical processes. Hydrometall. 98 (1–2), 1–9.

Zhao, K., Gao, F., Yang, Q., 2022. Comprehensive review on metallurgical upgradation processes of nickel sulfide ores. Journal of Sustainable Metallurgy 8 (1), 37–50.

Zheng, X., Zhang, L., Fan, Z., Cao, Y., Shen, L., Au, C., Jiang, L., 2019. Enhanced catalytic activity over MIL-100 (Fe) with coordinatively unsaturated Fe2+/Fe3+ sites for selective oxidation of H2S to sulfur. Chem. Eng. J. 374, 793–801.

Zuo, Y., Chen, Q., Li, C., Kang, C., Lei, X., 2019. Removal of fluorine from wet-process phosphoric acid using a solvent extraction technique with tributyl phosphate and silicon oil. ACS Omega 4 (7), 11593–11601.